Cold Regions Science and Technology 217 (2024) 104029

Contents lists available at ScienceDirect

Cold Regions Science and Technology

journal homepage: www.elsevier.com/locate/coldregions

Sea-spray measurement tools and technique employed in marine icing field expeditions: A critical literature review and assessment using CFD simulations

Sushmit Dhar [a,*], Masoud Naseri [a], Hassan Abbas Khawaja [b], Eirik Mikal Samuelsen [c,d], Kåre Edvardsen [b], Javad Barabady [a]

[a] Department of Technology and Safety, UiT The Arctic University of Norway, Tromsø, Norway
[b] Department of Automation and Process Engineering, UiT The Arctic University of Norway, Tromsø, Norway
[c] Meteorological Institute, Norway
[d] Department of Physics and Technology, UiT The Arctic University of Norway, Tromsø, Norway

ARTICLE INFO

Keywords:
Sea-spray icing
Sea-spray measurement
Sea-spray flux
Field measurements
CFD

ABSTRACT

Sea-spray icing resulting from sea spray droplets accreting on exposed surfaces poses a significant safety concern for vessels and marine structures operating in cold climate regions. One of the key parameters determining the amount of ice accretion is the quantity of incoming sea spray, which eventually comes in contact with the structure in the presence of brine film freezing temperature. Hence, to develop marine icing estimation models, researchers have been inclined towards conducting field measurements to acquire data on sea spray and its key characteristics, such as liquid water content (LWC, mass of spray water per unit volume of air), spray frequency and duration, and droplet size distribution. This paper provides a critical review of various techniques used by researchers for sea spray field measurements. By employing Computational Fluid Dynamics (CFD) simulation, this paper also evaluates the performance of instruments for measuring sea-spray flux employed in such field campaigns. Design issues and potential areas for improvement are identified and discussed, based on which further recommendations for improvement of sea spray data collection are provided. The study provides valuable insights for researchers planning field measurement expeditions and exploring viable options to design an efficient system for collecting sea spray data.

1. Introduction

For decades, sea-spray icing has been a well-known problem adversely affecting vessels operating in cold regions (Shellard, 1974). Regardless of the type of vessel or structure, spray icing has the potential to be hazardous. Ice accumulation may hamper the safety of the operators, affect manoeuvrability, or damage critical pieces of machinery onboard. The effect may be detrimental, especially for smaller vessels, such as fishing vessels with lower residual stability, where the building of topside icing due to freezing sea spray may rapidly lead to a negative metacentric height (GM), impairing the stability of the vessel and eventually resulting in capsizing (Chung, 1995). The sinking of the fishing trawlers "Lorella" and "Roderigo" north of Iceland in January 1955, attributed to icing, served as a catalyst and drew attention to the inherent dangers associated with this phenomenon and marked the beginning of research on the topic (Blackmore and Lozowski, 1993; Hay, 1956). Despite the passage of time, reports of catastrophic incidents resulting from ice accumulation in recent years, such as the capsizing of fishing vessels Destination in February 2017 (NTSB, 2018) and Scandies Rose in December 2019 (NTSB, 2020) in the Bering Sea and the capsizing of fishing trawler ONEGA in December 2020 in the Barents Sea (Dhar et al., 2022), continue to emphasise the importance of addressing this issue.

Forecasting icing events and estimation of icing rates are vital for studying the risk of ice build-up. With improvements in marine icing prediction models and warning systems, operators in the region may take preventive actions and have the possibility to plan their tasks accordingly. The formation of ice on structures is primarily determined by the heat exchange between the surrounding environment and the liquid water available to freeze (Samuelsen, 2017). Therefore, to

* Corresponding author.
E-mail address: sushmit.dhar@uit.no (S. Dhar).

https://doi.org/10.1016/j.coldregions.2023.104029
Received 26 July 2023; Received in revised form 19 September 2023; Accepted 22 September 2023
Available online 24 September 2023

accurately estimate marine icing, it is important to know the spray flux at the location of icing calculations.

In order to model the intricate process of spray generation, researchers usually break the process down into its components. This involves analysing the events based on droplet size and other crucial input parameters for icing estimation models such as the LWC (required to calculate the spray mass flux), the frequency of spray generation, and the duration of exposure of the marine structure to the spray cloud during a spray event (Mintu and Molyneux, 2022).

There are various types of icing models available that employ different approaches for utilising the spray models to estimate icing, which can be categorised as follows: (1) Fully stationary models such as RIGICE (Roebber and Mitten, 1987) and MINCOG (Samuelsen et al., 2017), where a constant spray mass flux input is applied throughout the entire icing period. (2) Quasi-steady models, such as the Midgett model (Lozowski and Zakrzewski, 1993; Lozowski et al., 2000), are characterised by changing spray mass flux input. (3) Fully time-dependent models such as ICEMOD (Horjen, 1990, 2013, 2015). In a model of category (1), it is not necessary to use the spray frequency and duration, and the time-average spray mass flux can be employed directly. However, in cases where LWC is used, all three model categories will require spray frequency and duration as input.

In general, three main approaches have been applied for the research on sea spray related to icing: laboratory experiments, simulations, and field measurements.

Attempts were made to generate wind-generated sea spray and quantify the flux in laboratory wind-wave tanks (Toba, 1962; Lai and Shemdin, 1974). However, such studies often produced discrepancies when compared to field studies (Monahan, 1968; Preobrazhenskii, 1973; Wu et al., 1984) primarily due to the difference in fetch, which creates considerably higher roughness in the field than in laboratory conditions. Additionally, humidity levels are near saturation in the field, while the laboratory environment is less humid (Itagaki, 1984). There have been a few attempts to analyse spray generation through scale-model experiments. Chung et al. (1998) performed scale-model experiments using a 1:13.43-scale model of the stern trawler Zandberg in a towing tank to generate impact-generated spray. However, the spray droplets were not suitably scaled, and this produced unrealistically large droplets at full-scale. In a 1:36-scale model experiment on an FFG-7 class combat ship, Sapone (1990) utilised surfactant to lower the surface tension. Despite the effort to scale down the critical spray properties, the water Weber number was still significantly smaller than the full-scale requirement (Mintu et al., 2021a). A 1:30-scale model experiment was conducted to replicate the full-scale measurements of spray events at Tarsuit Island (Muzik and Kirby, 1992). In order to match the droplet size with full-scale measurements, wind velocity was not scaled. Spray data was collected by measuring water volume deposited over half of the model island and then doubled to estimate the total spray overtopping volume. Results showed laboratory values of the spray volume were almost three times higher than those in the field, where the spray was collected in drums. The discrepancy is attributed to the scaling effects of the wind speed in the model study, data collection method variation, and differences in average wind speeds between the field observations and the model study.

Additionally, a few numerical simulations (Mintu et al., 2019) and theoretical models (Dehghani et al., 2016a, 2016b, 2018) have been utilised to simulate and analyse the characteristics of wave-impact sea spray. Notably, computational fluid dynamics (CFD) techniques, such as the smooth particle hydrodynamics method, have also been introduced to simulate wave-generated sea spray (Mintu et al., 2021b; Chen et al., 2022). Nevertheless, these methods are accompanied by several assumptions and limitations. One of the main challenges lies in using the appropriate droplet size to accurately capture the intricate dynamics of a fine spray cloud, which currently exceeds the computational capabilities of GPU-accelerated or extensive parallel CFD software packages (Mintu et al., 2021b).

Given the limitations associated with the laboratory and simulation approaches, researchers have often emphasised the importance of collecting sea-spray data from the field for developing or calibrating accurate icing models. The spray pattern and droplet trajectory generated under a given set of meteorological and oceanographic conditions are influenced by various factors such as the shape, size, loading, manoeuvrability, speed, and heading of the hull or structure relative to the waves and the wind (Bodaghkhani et al., 2016; Kulyakhtin et al., 2016). These factors result in variations in the incoming spray flux for different ship types and marine structures, ultimately impacting the extent of ice accretion. As a result, empirical formulae developed from observations of specific ships or structures may exhibit uncertainty when applied to different ship types or marine structures (Roebber and Mitten, 1987; Sultana et al., 2018). Therefore, it is desired to collect spray data from multiple ships and structures for an extended period in order to develop a robust icing model (Samuelsen and Graversen, 2019).

Several field expeditions have been conducted on various ships (Tabata, 1969; Horjen et al., 1986; Borisenkov et al., 1975; Ryerson and Longo, 1992; Ozeki et al., 2018; Teigen et al., 2019), offshore structures (Jorgensen, 1986, 1985, 1984; Minsk, 1984), and on islands (Muzik and Kirby, 1992; Andreas, 2016) to gather field data on sea spray. A range of instruments has been employed to measure sea-spray flux and important components of sea spray for the development of icing models, including unconventional items like toilet paper rolls (Tabata, 1969) and baby diapers (Jorgensen, 1984), as well as specialised instruments like the cloud imaging probes (CIP) (Andreas, 2016) and high-speed camera (Jorgensen, 1984).

Collecting field data on sea spray in cold regions can be challenging in terms of logistics, required technology, cost, and safety considerations, particularly due to the harsh conditions associated with cold temperatures, including heavy seas and strong winds. The information on previous field expeditions has been scattered across various sources, many of which are difficult to access and/or written in non-English languages, such as reports on measurements conducted on Japanese patrol boats between 1963 and 1967 (Tabata, 1969) written in Japanese and measurements on the drilling rig Treasure Scout (Jorgensen, 1984) written in Norwegian. Moreover, to the best of the authors' knowledge, a study that provides a thorough, systematic, and critical review and analysis of the literature regarding the instruments and techniques utilised in such expeditions is currently lacking.

The objective of the current study is to provide a comprehensive overview of field expeditions undertaken for sea-spray data collection, emphasising the deployed equipment, addressing encountered challenges and design issues, and identifying potential areas for improvement. This study also employs CFD as a numerical simulation method to evaluate the efficiency of the sea-spray flux measuring instruments used by the researchers during the field expeditions to gain qualitative insight into their performance without the need for physical testing. In order to achieve this, we used computer-aided design (CAD) models to recreate the geometry of the instruments according to descriptions provided by the researchers. These models were then run on ANSYS® Fluent CFD software. The CFD solver is based on the Reynolds-averaged Navier-Stokes (RANS) equations with the k-ω Shear Stress Transport (SST) turbulence model. The simulations mimic a wind tunnel experiment to analyse the fluid flow characteristics around the instruments. The results of the analyses are further used to assess the advantages and constraints of the existing techniques for measuring sea-spray flux. The overall study provides a practical resource for researchers planning field measurement expeditions for collecting sea spray data, enabling them to explore suitable options to devise an efficient system for their specific

needs.

The subsequent sections of this paper are organised as follows: Section 2 provides a review of field expeditions for collecting sea-spray data; Section 3 outlines the CFD methodology used to assess the efficiency of spray flux measuring devices; Section 4 analyses the performance of these devices; Section 5 discusses the measurement methods for different sea spray parameters and provides device evaluations and recommendations for future designs; Section 6 presents the concluding remarks.

2. Field measurements

This section provides a historical review of field expeditions that collected data on sea spray with the primary objective of developing or calibrating models for estimating marine icing.

2.1. Sea spray measurement onboard Japanese patrol boats

According to the available literature, Tabata (1969) provides the earliest documented record of sea-spray measurement, highlighting two distinct methods. The first method involved gathering reports from patrol boats operating in icing waters between 1963 and 1967, where meteorological and oceanographic conditions were recorded alongside the amount of sea spray and ice accretion. The information was gathered from 256 surveys completed by twelve boats of different sizes that were operating in the water nearby Hokkaido, Primorsky Krai, the Kuril Islands, and the Kamchatka region. The spray quantity was estimated based on the extent, specifically reaching the bridge window, and was categorised into three levels: no spray, moderate spray, and heavy spray. Based on the survey findings, it was concluded that icing initiation occurred at air temperatures below −2 °C, relative wind speeds of 6–8 m/s or higher triggered icing, and ice accretion intensified with slight changes in wind speed or temperature. The relative angle between the wave and ship heading was identified as a crucial factor in icing, as with smaller angles, smaller ships, or higher wave heights resulting in increased sea spray observations (Itagaki, 1977).

The second type of measurement was carried on the 350-metric-tonne patrol vessel “Chitose”, using a sea-spray collector (Fig. 1 (a)) consisting of a water-absorbing cylinder made of toilet-paper roll and wind cups. Ten devices were installed on the upper deck positions (Fig. 1 (b)), and measurements were conducted on 30 July 1964 outside Wakkanai Port. The water-absorbing cylinders were removed at intervals of every five to six minutes during spray events, placed in polyethene bags, and weighed upon arrival at the port. Measurements were taken at different headings relative to the waves, with angles of 0°, 30°, and 60°, and at vessel speeds of 12.5 knots and 10.7 knots. Despite the moderate weather conditions prevailing during the measurements, variations in sea-spray flux were observed based on the relative angle and speed.

2.2. Spray measurements on medium-sized fishing vessels by soviet researchers

During the 1960s–1970s, Soviet researchers extensively studied marine icing, particularly on medium-sized fishing vessels (MFVs). The research included field observations, device development, laboratory experiments, estimation models, and de-icing techniques. Zakrzewski carefully reviewed reports and journals and extracted essential information (Zakrzewski, 1987, 1986; Zakrzewski and Lozowski, 1989). Nevertheless, still much of the information remains inaccessible and vague. The researchers conducted various studies to investigate the collision-generated spray, including the spraying zone of a ship (Buyanov, 1971; Kultashev and Panov, 1970; Kuznietsov et al., 1971; Sharapov, 1971; Smirnov, 1972), frequency of spraying (Aksyutin, 1979; Kultashev et al., 1972; Panov, 1976, 1971), and LWC and droplet size distributions (Borisenkov, 1972; Borisenkov et al., 1975; Borisenkov and

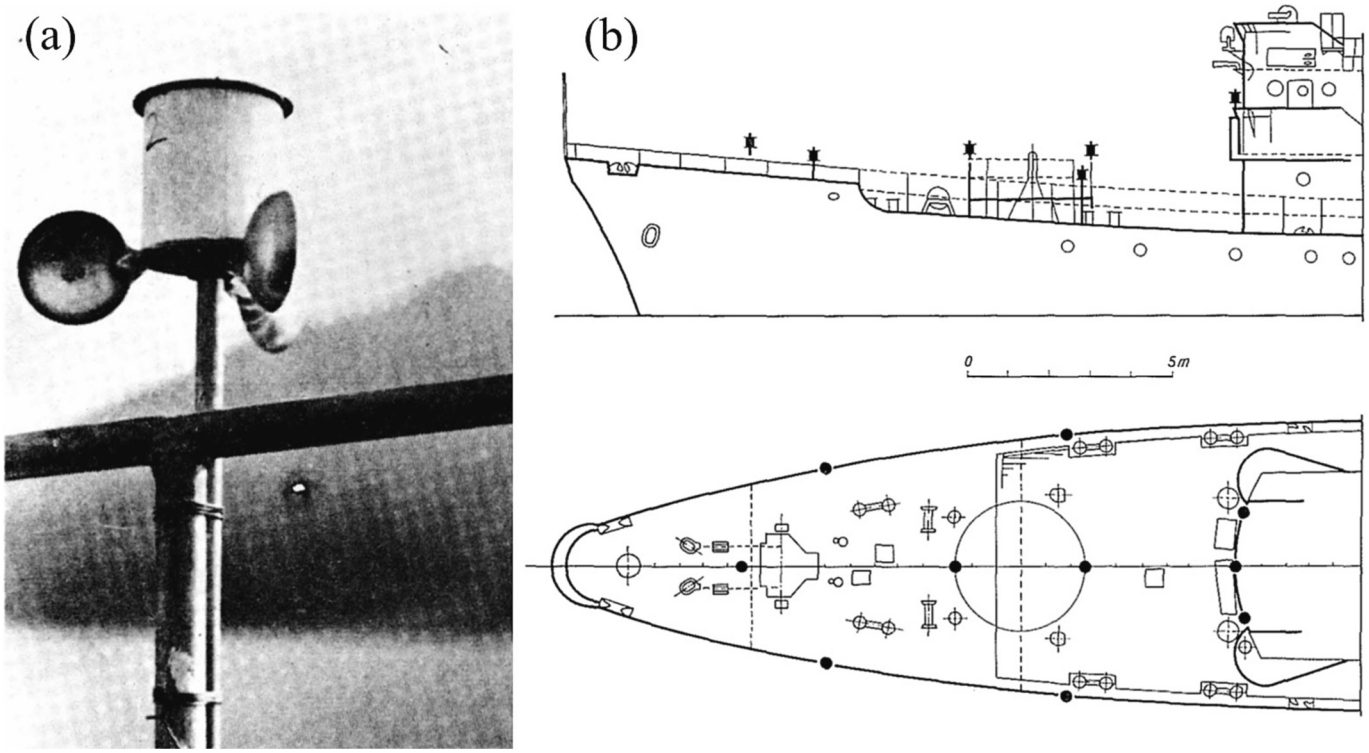

Fig. 1. (a) Sea-spray collector device consisting of absorption cylinder made of toilet paper rotated by wind cups; (b) locations of the device installed onboard patrol vessel “Chitose” (Tabata, 1969).

Panov, 1972). Based on the available information, it can be ascertained that the spraying zone and spray frequency were primarily obtained through visual observations. Spray cloud parameter measurements of LWC and droplet size were carried out on two Soviet ships, namely the MFV Iceberg and MFV Narva. However, only limited details are available concerning the specific instruments and methodologies employed during these field expeditions.

Research of Gashin (Borisenkov, 1972; Borisenkov and Panov, 1972) focused on the observations made on MFV Iceberg between August and November 1969 in the Atlantic Ocean. The study states that collision-generated droplets measured were in the range of diameter 1.0 to 3.5 mm, with an average size of 2.4 mm. The mean duration of a spray event was around 2 s. The average values of the LWC were presented during one spray event for different locations on horizontal and vertical surfaces at different wind speeds ranging from 0 to >15 m/s and heading angles relative to waves of 0–90°. The data showed water content of the spray clouds gradually decreased to the midship part and with increased heights over the deck. The wave height is considered the main factor for determining the incoming LWC. The amount of spray was also greater at wave heading angles of 30–60°, and it increased with increasing wind speed. Under certain wave conditions, the spray flux on horizontal and vertical surfaces varied within the range of $0–3{\cdot}10^{-2}$ g/cm^2/s. Spray formation was more pronounced in wind wave conditions, which resulted in more spray entering the ship.

Measurements on MFV Narva were carried out in February 1973 in the Sea of Japan (Borisenkov et al., 1975). The field expedition involved collecting approximately 50 samples from the spray cloud at various points on the deck and at multiple levels. The measurements were conducted under air temperatures varying from 2 to 6 °C, sea-surface temperatures ranging between −1 and − 0.8 °C, sea states classified as 5 to 6, wind speeds ranging from 10 to 12 m/s, and a heading angle relative to the wave between 70° and 90°. The spray droplet size distribution was determined by trapping droplets using a soot and viscous oil mixture (1:3 weight ratio). The mixture was applied on a metal substrate with a 5–10 mm thickness, aligned perpendicular to the spray propagation. The trapped droplets made distinct imprints, with each imprint reflecting the diameter of the corresponding droplet. Additionally, the droplet spectrum was measured using absorbent and colouring substrates. The arithmetic mean droplet diameter on viscous substrates was 0.49 mm, while on absorbent substrates, it was 0.84 mm with a maximum droplet size of 3–4 mm.

LWC measurements were conducted at the height of 0.7–4 m from the deck, using special traps designed by the Leningrad Polytechnic Institute. However, no information about the design or construction of the traps was provided. The spray cloud propagation velocity was determined to be 6 m/s, with a duration of 5.8 s which was measured using a high-speed camera. The total water content of the spray cloud above the MFV deck was estimated to be around 300 l per spray event.

Some studies regarding wind-generated spray have also been conducted. Preobrazhenskii (1973) measured the vertical distribution of LWC of wind-generated spray at 1.5, 2, 4, and 7 m above the sea surface from a ship in moderate to high winds (7–25 m/s) (Wu, 1990). Spray droplets were collected on 10–20 mm oil-coated glass slides. The slides were fixed to a boom, which extended about 3 m from the bow of the ship, cruising slowly into the wind. The droplet impressions on the plates were counted and sorted size-wise. It was deduced from the measurements that the net droplet volume diminished with height. The data shows that spray droplets exceeding 30 μm in diameter may reach heights above 7 m when wind speeds exceed 12 m/s, while droplets larger than 100 μm reach that height when wind speeds surpass 25 m/s. Gashin registered wind-generated droplets size ranged between 60 μm – 1 mm during the MFV Iceberg expedition (Borisenkov and Panov, 1972). Also, during the MFV Narva research expedition, about 30 samples of wind-generated spray were collected to determine the spectrum of droplets at the height of about 1 m above sea level (Borisenkov et al., 1975). The minimum droplet size that was possible to be measured by their technique was 0.08 mm in diameter. According to the data, the average droplet diameter of wind-generated spray was 0.25 mm, and the maximum was approximately 1.2 mm.

2.3. Spray measurements on Tarsiut Island

Muzik and Kirby (1992) provide a description of the spray measurements carried out during the 1982 open-water season on Tarsiut Island, an artificial caisson-based island (Fitzpatrick and Stenning, 1983) in the Beaufort Sea (Fig. 2 (a)). The measurements aimed to evaluate the horizontal distribution of sea spray on the island and estimate the spray volume generated from the impact of waves during high winds and wave events.

The spray amount on the island was collected using 45-gal drums (0.56 m diameter x 0.8 m high) by placing them in the proximity of the wind (Fig. 2 (b)). Spray level was logged hourly during some strong weather events (see Table. 1) and half-hourly during event peak. During the “middle of the event” period, spray generation was observed for every third or fourth wave in the wave train, while during the “peak of the event”, spray landing on the island occurred approximately for every second wave. A scaled model study was also conducted in the laboratory for comparison. As mentioned earlier in Section 1, the field results of

Fig. 2. (a) Tarsiut Island, Beaufort Sea (Picture R. R. Ward). (b) Typical layout of measuring drums (black dots numbered) on the island during the field study (Muzik and Kirby, 1992).

Table 1
overview of wind, wave, and spray data measured on Tarsiut Island (Muzik and Kirby, 1992).

Date	Maximum recorded significant wave height (m)	Maximum recorded spray rate (cm/h)	Average wind speed (m/s) *	Maximum wind speed (m/s)
20, 21 August 1982	2.5	61	16.6	18.9
6,7,8 September 1982	2	31	10.6	17.3
17 September 1982	1.75	6	5.1 (estimated)	5.1 (estimated)

* Measured at a height of 34 m.

spray overtopping volumes were found to be one-third of the comparable model results.

Collected data on Tarsiut Island were utilised by Lozowski et al. (2002) to improve the LWC and the spray frequency algorithm (based on probability distribution of wave heights producing spray) for the RIGICE model, which was developed to compute ice loads on drilling rigs in Canadian waters. Forest et al. (2005) later claimed to improve this model to RIGICE04, also by using these spray data to develop a new LWC and spray frequency algorithm.

2.4. Spray measurements for ICEMOD

The "Offshore icing" research program launched in 1983 aimed to improve understanding and estimation of icing on offshore structures and vessels through field data collection, wind tunnel experiments, and the development of the icing model ICEMOD (Horjen, 1990; Horjen and Vefsnmo, 1987) (originally called ICING (Horjen and Vefsnmo, 1984)) and its subsequent versions (Horjen, 2015, 2013).

2.4.1. Spray measurements on offshore platforms

Jorgensen (1984, 1985, 1986) describes six field data collections conducted on the Treasure Scout drilling rig from April 1983 to December 1984. Measurements were also made on the Edda platform from September 1985 to January 1986.

Specialised instruments were developed to collect spray characteristics data on LWC and droplet sizes. Absorbent panels made of disposable baby diapers (Fig. 3 (a)) were used to measure the spray LWC because of their high soaking capacity. These diapers were held in place by a rectangular plexiglass holder (25 cm × 10 cm) with clamps for attachment to railings or similar structures, secured by netting. Another designed equipment was the pipe bend collector (Fig. 3 (b)), consisting of a 10 cm diameter bent plastic pipe with a glued-on transition cone and a graduated measuring gauge made of plexiglass. The collector, attached with a clamping device, allowed for the collection of spray, with a valve at the bottom of the measuring gauge for emptying the collected spray.

The panels and collectors were positioned in various locations below the main deck, and spot measurements were carried above the main deck. The positions of the instruments were constantly changed depending on the wind direction. The water absorbed by the diapers was weighed before and after exposure using a spring balance, while the water collected by the pipe bend collectors was directly read in millilitres on the graduated measuring glass. Measurement readings were omitted during precipitation, and experimental corrections were applied to account for evaporation.

A photographic technique was developed to record droplet sizes in a spray cloud (Jorgensen, 1983). Parts of the droplet cloud passed through an open box at the end of the long tube attached with a powerful flash. The flash was triggered manually when a sea spray hit the box. The droplets passing in front of an illuminated plate were photographed by a motor-driven camera placed in a waterproof case above the open box (Fig. 4).

Two observers visually recorded the sea spray frequency by counting the occurrences of spray events elevating 2 m above the waterline level during 10-min intervals, and the average of their observations was used to calculate the spray frequency. Simultaneously necessary meteorological data was recorded from the weather station on the rig or estimated visually.

2.4.2. Spray measurements on vessels

Sea-spray measurements were carried out on four vessels: Troms Tjeld, Tender Turbot, Tender Trout, and Endre Dyrøy, with the findings detailed by Horjen et al. (1986).

Horizontal spray flux was measured using seven pipe bend collectors at different heights (10.2 m, 11.3 m, and 13.8 m above sea level) on the sister ships Tender Turbot and Tender Trout. Flux measurements showed no significant difference between the upwind and leeward sides of the ship. As wind strength increased, spray fluxes also increased. The measured frequencies varied between 0.3 and 1.25 per minute at a reference height of 10 m above sea level. Droplet sizes were captured using the photographic technique, on the bridge deck at the height of 10

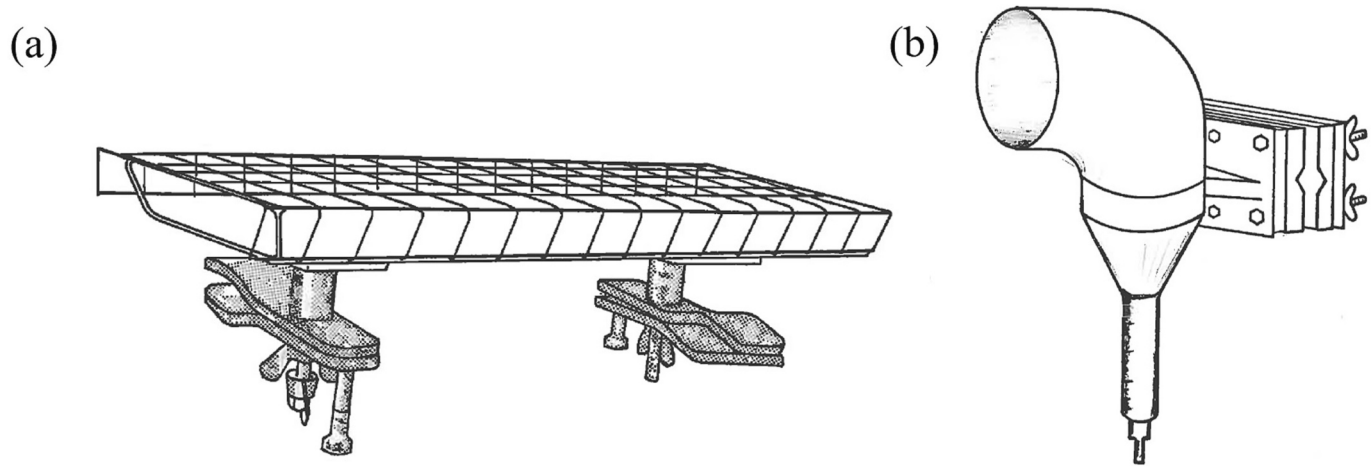

Fig. 3. (a) Absorbent panel made of baby diaper; (b) pipe bend collector (Jorgensen, 1984).

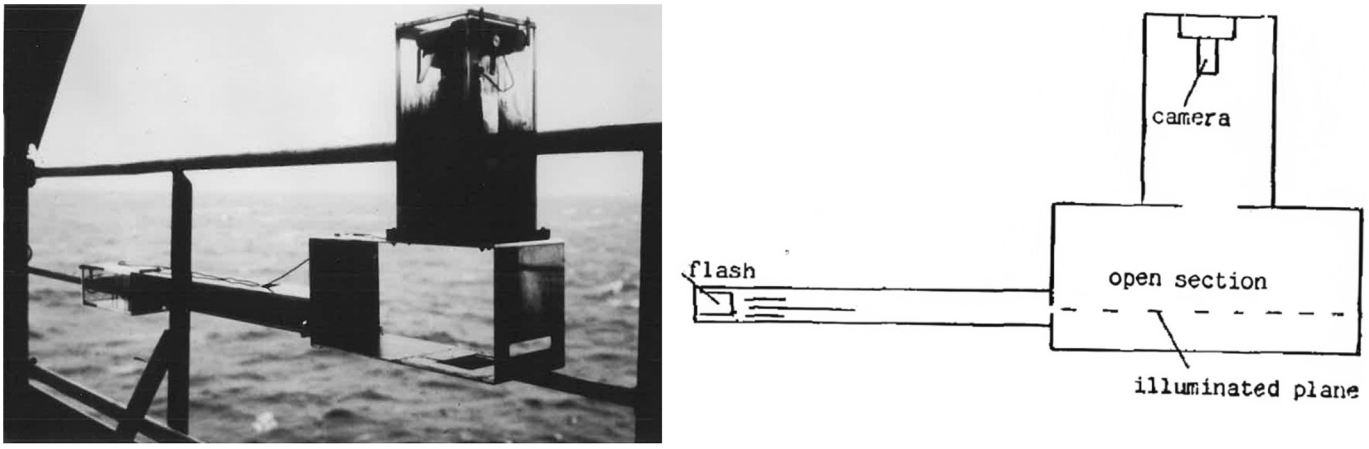

Fig. 4. Picture and schematic of the photographic technique used to measure droplet size (Jorgensen, 1984, 1986).

m, with droplets ranging from 0.0 to 5.5 mm.

Spray flux was measured on the vessel Endre Dyrøy using pipe bend collectors positioned at heights on the mast (6.6 m, 7.5 m, 9.1 m, and 10.9 m above sea level). The spray flux exhibited an exponential decrease with increasing height, while the vessel speed showed no significant impact. Spray flux also increased with heading within the range of 0°-45°.

On the vessel Troms Tjeld, spray flux was measured with six pipe bend collectors attached to different locations and heights (4.95 m, 9.95 m, and 11.65 m above sea level). The measurements indicated a strong correlation between the spray flux and significant wave height. The average spray frequency was measured to be three sprays per minute that reached the wheelhouse.

2.5. Spray measurement on the USCGC Midgett

Ryerson and Longo (1992) provides an overview of the measurements aboard the U.S. Coast Guard Cutter Midgett, a 115 m Hamilton-Class high endurance cutter, carried out by Cold Regions Research and Engineering Laboratory (CRREL) between 5 February and 13 March 1990. The objective was to gather empirical data on spray delivery and superstructure icing in the Gulf of Alaska and the Bering Sea.

The details of the various equipment that was designed for the expedition is provided by Walsh et al. (1992). A spray icing unit (SIU) illustrated in Fig. 5. was designed as a stand-alone system to autonomously collect spray and icing data. The unit mainly comprised spray flux and ice thickness measuring equipment, a data logger control system, and pneumatic and battery power supplies housed in a rectangular box weighing approximately 250 kg. The CRREL horizontal separator interceptor (Fig. 5 (a)) was designed for collecting spray flux in the horizontal direction, and for vertical spray flux (Fig. 5 (b)), a vertical spray collector was designed. A total of six SIUs were installed on the ship at various distances from the bow and at different heights (port and starboard main deck and 02 level bulkhead surfaces, and on 01 level and flying bridge deck surfaces).

The CRREL horizontal spray interceptor is a flow-through design that uses the principles of momentum and coalescence to separate spray droplets from the air stream. The air-borne droplets enter the separator through the inlet and are redirected around a convex baffle. The large droplets, due to their momentum, collides with the baffle and separate from the air stream and fall into the measuring tank. After passing the baffle, the air stream enters the chamber twice the size of the inlet. The smaller droplets, which were not separated at the baffle, then impact and coalesce around a mesh screen behind the baffle in this chamber. As these droplets coalesce and become heavy, they run down the screen and are collected in the tank. The accumulated spray is measured by a

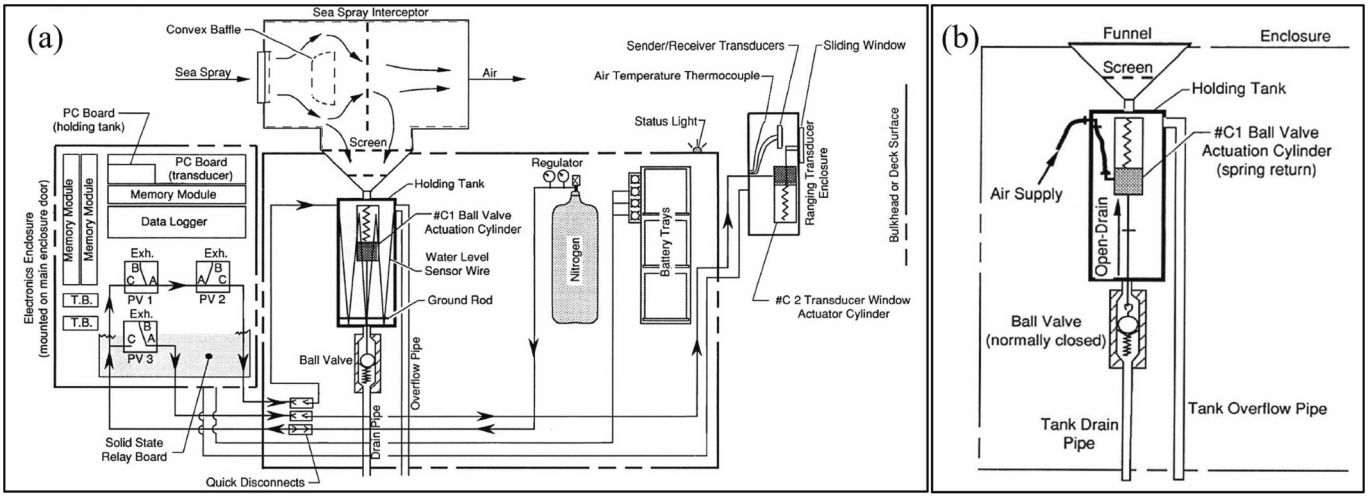

Fig. 5. (a) Schematic of CRREL horizontal spray interceptor mounted on the SIU; (b) schematic of CRREL vertical spray collector (Walsh et al., 1992).

Table 2
Vessel specifications of the USCGC Midgettt and USS Monterey (Thomas, 1991).

	USCGC Midgettt	USS Monterey
Displacement (t)	3065.40	9752.02
Length between perpendiculars (m)	106.68	161.24
Beam (m)	12.8	16.76
Draft (m)	4.26	6.1
Freeboard (m)	7.92	9.45

capacitance change detector circuit fitted inside the measuring tank. The tank drain is connected to a ball check valve which is triggered by a pneumatic cylinder. A Campbell CR10 data logger is used to store data and, as a controller, is programmed to activate the pneumatic cylinder for 10 s to drain when full. The data logger store one water level reading every second by averaging 12 sample readings.

The CRREL vertical collector is similar to the rain gauge, consisting of a funnel with a diameter of 30 cm diameter with a debris screen. The funnel is connected to an 11.6-l holding tank. Alongside it, two Young automatic rain gauges (Model 50,202, RM. Young *Co.*) were installed on the SIUs, while two standard manual rain and snow gauges (Model 6310-A, Qualimetrics, Inc.) were placed adjacent to enable a comparison of the vertical spray flux measurements.

Sea-spray measurements were only made when air temperatures were above freezing as no heating element was not installed due to limited power availability by the batteries. When the temperature dropped below freezing, the controller disabled the spray collection system and opened the drain valve.

Two cameras equipped with wipers and freshwater washers were mounted on the flying bridge with a clear view of the bow. The collected footage was analysed to estimate the duration and characteristics of spray events, and it was also used to confirm the spray events by comparing the collected data with video images of the events. A universal flying particle camera, which is a stroboscopic video system, was used to measure the sizes of droplets in the spray cloud.

Ryerson (1995) provides detailed information on 39 spray events during the expedition, including information on the spray duration, the number of drops per cubic meter, droplet diameter, LWC, spray flux, the ship speed, and wind and wave parameters. The duration of the spray event ranged between 0.47 and 5.57 s, with an average of 2.73 s. The concentration of droplets in most spray clouds ranged from 2.0×10^5 to 3.0×10^5 drops/m^3. The sizes of the droplets in the spray clouds ranged from 14 to 7700 μm in diameter, with a median of 234 μm. The LWC of the spray clouds varied between 1.1 and 1162.9 g/m^3, with an average of 64.1 g/m^3.

2.6. Spray generation measurement on USCGC Midgett and USS Monterey

Thomas (1991) conducted full-scale ship trials to investigate the relationship between ship motion and bow spray generation. Measurements were conducted onboard the USCGC Midgett in the Bering Sea in 1990 and on the USS Monterey in the northwest North Atlantic Ocean in 1991. Ship motions were recorded using a Ship Motion Recorder (SMR) and a tri-axial accelerometer package. Bow spray events were captured using video camera systems mounted on the forward superstructure of the vessels. Each trial measurement involved maintaining a constant heading and speed for 20 min, with the number of observed bow spray events recorded during this period. Table 2 presents the specifications of the vessels during the expedition.

Analysis revealed a strong correlation between bow spray occurrence and ship pitch and vertical acceleration. No significant relationship was found between roll motions and bow spray generation. In the absence of significant ship motions at the bow, spray clouds across the bow could not be generated by wind alone, although differences in total sprays were attributed to variations in true wind speed. The data indicated specific threshold values for pitch and acceleration for spray generation, which were smaller for the Midgett (pitch $>1.06^\circ$ and the vertical acceleration > 0.19 g) compared to the Monterey (pitch $>1.46^\circ$ and the vertical acceleration > 0.22 g), which is expected given the larger size and greater freeboard of the Monterey. However, large vertical accelerations did not always result in spray events, suggesting the importance of considering both vertical acceleration and the relative ship-wave position for predicting spray events.

2.7. Sea-spray measurements using SPC and MRS

Ozeki et al. (2016) mention the development of two gauges, the Spray Particle Counter (SPC) and Marine Rain gauge type Spray gauge (MRS), for measuring sea spray droplets size distribution and the spray amount.

The SPC (SPC-S7, Niigata Denki *Co.*), illustrated in Fig. 6 (a), was initially developed to measure drifting snow (called Snow Particle Counter) but was later modified to count sea spray droplets. The sensor unit has a Super-Luminescent Diode (SLD) oriented in parallel rays measuring the light attenuation by passing droplets and has a sensing region of dimension 25 mm wide, 3 mm height, and 0.5 mm depth. The system is comprised of the sensor, data processor, and personal computer.

The marine rain gauge type spray gauge (MRS) illustrated in Fig. 6 (b) consists of an automatic rain gauge Young model 50,202 for vertical spray flux measurements and a cylindrical trap fitted above to block

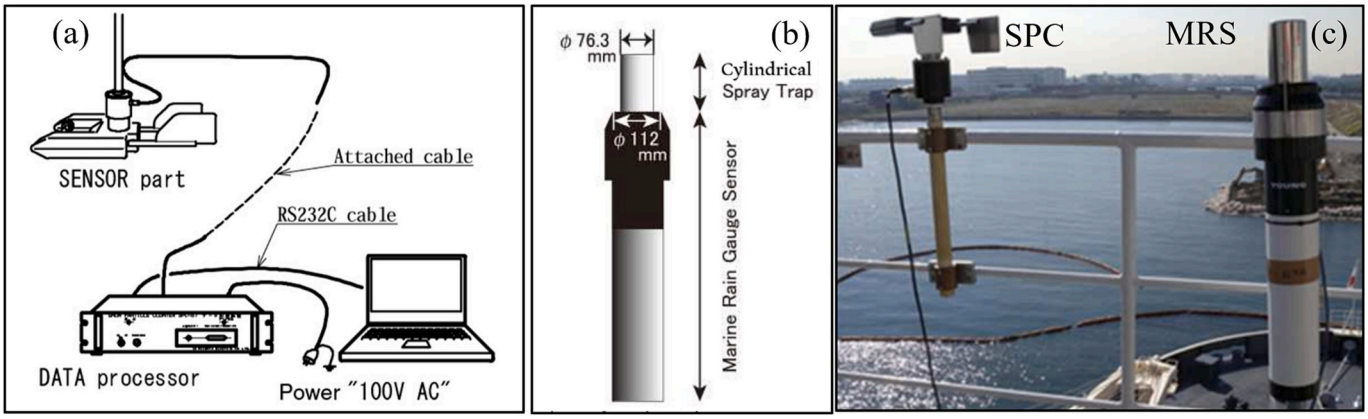

Fig. 6. (a) Schematic diagram of SPC; (b) schematic diagram of MRS; (c) SPC (Left) and MRS (Right) mounted on a vessel (Ozeki et al., 2016).

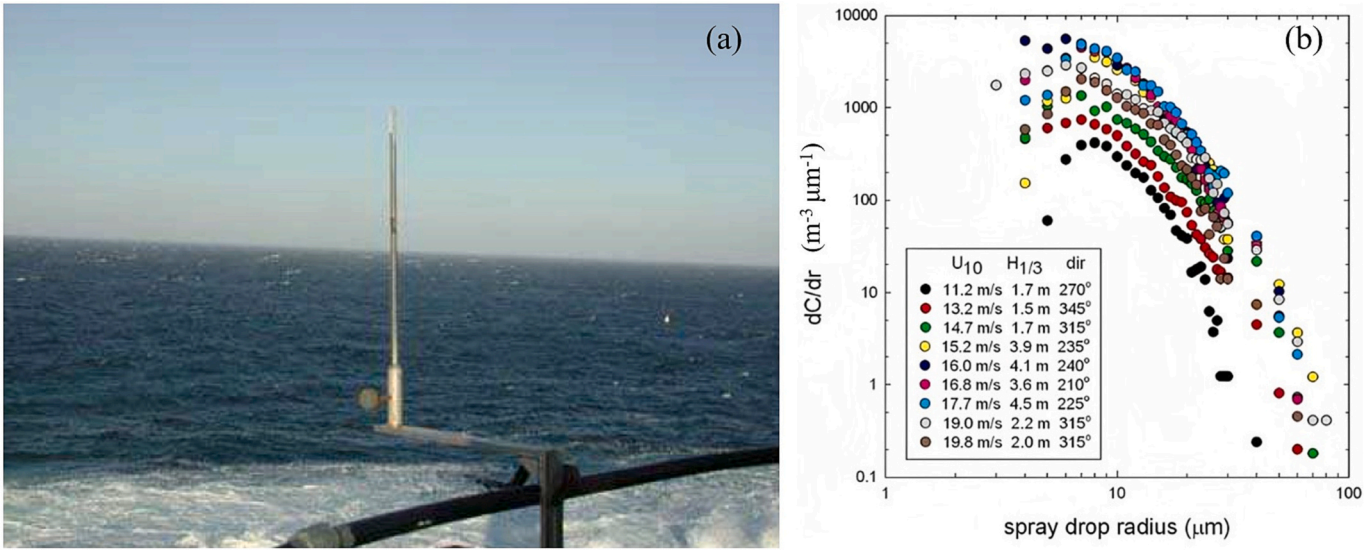

Fig. 7. (a) Microscope slides attached to a support for collecting spray drops samples; (b) sea spray concentrations (dC/dr) of nine observations, along with the wind speed at 10 m (U_{10}) and significant wave height ($H_{1/3}$) and wind direction (dir) (Jones and Andreas, 2013).

Fig. 8. Cloud Imaging Probe (CIP) and the Sonic anemometer (Andreas, 2016).

Fig. 9. Rotating multicylinder mounted on Mt. Desert Rock lighthouse (Jones and Andreas, 2014).

spray in the horizontal direction. The cylindrical spray trap is 120 mm high and has a diameter of 76.3 mm and a projected area of 92 cm^2. The impinging spray impacts the trap and drains into the catchment funnel of the rain gauge. The data is recorded every minute with the smallest measurable unit of 1 mm.

Between 2012 and 2021, several expeditions were conducted that involved spray measurements on vessels using the two gauges (Fig. 6 (c)) across various locations, including the Arctic Ocean, Bering Sea, North Pacific region, and Antarctic Ocean region (summarised in Table 4). Though no specific spray flux formulae have been presented thus far based on the collected data (Ozeki, personal communication, 2022), the analysis shows a strong correlation apparent between the amount of sea spray generated and the relative wind velocity (Ozeki et al., 2016a; Shiga et al., 2015).

2.8. Spray measurements at Mt. Desert Rock

Sea-spray measurements were conducted on Mt. Desert Rock, located near the coast of Maine, USA. This island, chosen for its resemblance to artificial islands in the Arctic, serves as a representative location to measure wind-generated spray concentrations and generation rates. The collected data is potentially applicable in estimating spray icing on similar structures found in the Arctic region. The data collection method and results from the measurements made on the island are summarised in the following part.

Jones and Andreas (2013) describe the wind-generated spray data collected from December 2012 to January 2013. Microscope slides of 12.5 mm in width, coated with Vaseline to enhance hydrophobicity, were placed on the island lighthouse catwalk 20 m above sea level (Fig. 7 (a)). In order to capture the air-borne droplets, the slides were exposed for an hour to 2 min, depending on the wind speed. Then the slides were immediately photographed under a microscope and analysed using Image-Pro software. It is observed that the drop concentration is dependent on both the significant wave height and wind speed (Fig. 7 (b).

Andreas (2016) analyses the near-surface spray measurements conducted in January 2013 using a cloud-imaging probe (CIP) developed by Droplet Measurement Technologies, Inc. The CIP (Fig. 8) is an optical spectrometer equipped with 64 photodetectors that enables the counting and measurement of droplet size through optical imaging. The study provides data on spray droplet concentration and production rate for various wind speeds (5 to 17 m/s) and droplet radii ranging from 6.25 μm to 143.75 μm at a rocky shoreline. The findings reveal that spray concentration increases with the cube of wind speed while the shape of the concentration spectrum remains consistent across different wind speeds. Moreover, the near-surface spray concentration and production rate are significantly higher at the rocky shoreline compared to the open ocean, with a difference of three orders of magnitude.

Jones and Andreas (2014) reported measurements conducted between January and February 2014 to evaluate the spray concentration gradient formulation proposed by Fairall et al. (2009). They collected sea spray droplets simultaneously from two levels, 19 m and 7.5 m above sea level, using drop slides and a multicylinder device. While the drop slides had a limited sampling volume of 0.08 to 0.8 m^3, the multicylinder device (Fig. 9) was employed to supplement the data by sampling 10 s to 100 s of air volume (m^3) (Jones et al., 2014). The multicylinder works on the principle that the collision efficiency of wind-blown droplets on cylinders reduces with decreasing drop diameter. While the rotating multicylinder was developed to characterize drop distributions in supercooled clouds, it was modified to make measurements in the above-freezing conditions by using absorbent paper to cover each cylinder.

2.9. Sea-spray measurements on Norne FPSO

Teigen et al. (2019) provide a description of a device called the "Fluxmeter", designed under the project RigSpray for carrying real-time and autonomous measurement of sea-spray flux. Six fluxmeters were installed on the Norne floating production, storage, and offloading (FPSO) during the winter seasons of 2017–2018 and 2018–2019 (Fig. 10 (a)). The purpose of the measurement was to gather a dataset of spray measurements, meteorological data, and vessel motions to calibrate spray icing models for large ship-shaped offshore structures.

The RigSpray Fluxmeter (Fig. 10 (b) and 10 (c)) is a device designed to operate safely in environments with the potential for explosions (ATEX-compliant), making it suitable for installations in locations vulnerable to the risk of explosion due to the presence of fuel. It includes a video recording camera with a wide-view lens to monitor the bow region. The device features a collector plate of 0.5 m × 0.5 m dimension, and the instrument cabinet made of coated 5 mm thick steel, ensuring durability in harsh weather and sea conditions. Sea spray is collected on the collector plate and drained into a tipping bucket inside the cabinet through a hose. The water level in the tipping bucket is monitored by a Yokogawa wireless gauge pressure transmitter at a 1 Hz measurement frequency, and the data is transferred wirelessly. The tipping bucket automatically tips when the centre of gravity exceeds its rotation axis. After emptying the water, the bucket pivots back into its original position. The study results from this project are not publicly available as they are proprietary.

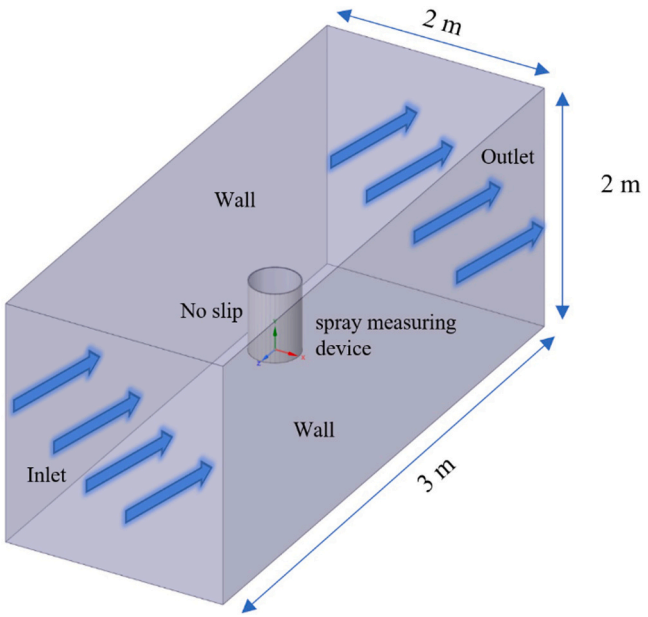

Fig. 11. The simulated wind tunnel setup.

3. CFD method

3.1. Sea spray droplets and stokes number

The Stokes number (*St*), which is a dimensionless number, is defined as the "ratio of the particle inertial relaxation time to the timescale characteristic of the turbulent flow" (Stokes, 1851; Veron, 2015). In the

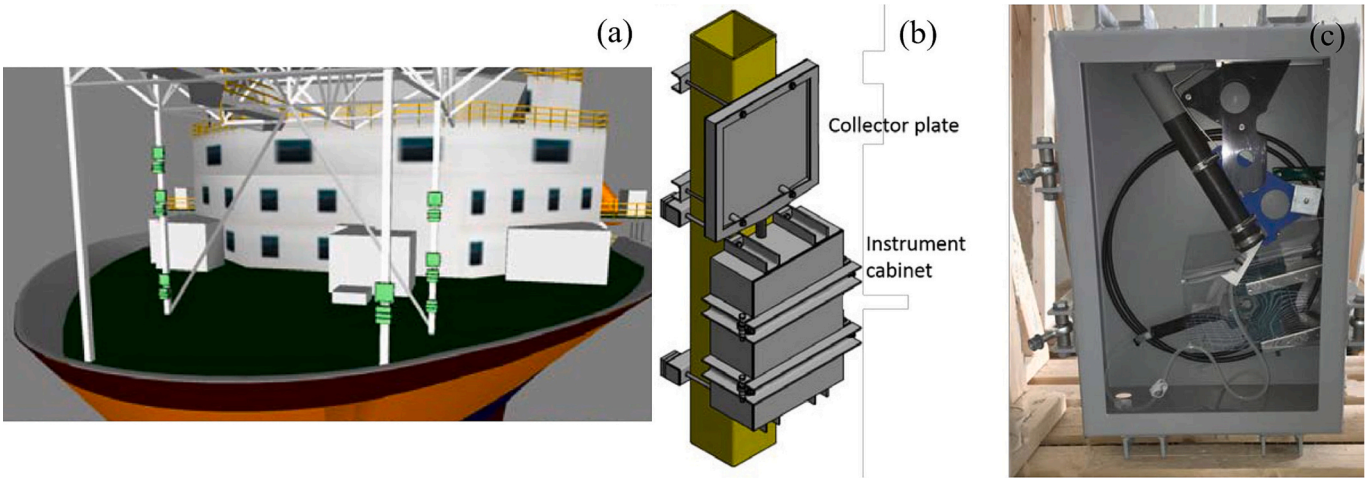

Fig. 10. (a) Locations of the six Fluxmeters mounted on FPSO Norne; (b) schematic diagram of the Fluxmeter; (c) instrument cabinet fitted with the tipping bucket and pressure sensor and transmitter (Teigen et al., 2019).

Table 3
Simulation parameters.

Model	Reynolds-averaged Navier-Stokes, steady-state, k- ω SST, isothermal, incompressible
Gravitational acceleration	9.81 m/s^2
Fluid Air (gas):	molecular mass 0.02896 kg/mol
Boundary conditions	wall (adiabatic, no slip)
Initial and ambient conditions	Pressure = 101,325 Pa, Temperature = 293.2 K
Free-stream wind speed along z	15, 30 m/s
Domain	length $z = 3$ m, width $x = 2$ m, height $y = 2$ m

context of sea spray, the trajectory of the droplets can be characterised by assessing their *St* by comparing their inertia to the fluid drag they experience in the airflow. When the *St* is low (i.e., $<< 1$), it indicates that the fluid drag is dominant, and the droplets will tend to follow the airflow trajectory and respond instantly to the fluctuations. On the other hand, when the *St* is high (i.e., $>> 1$), the droplets have significant inertia and follow their own inertial path and are less influenced by the surrounding airflow.

Based on previous measurements, the size of sea spray droplets varies between 0.02 μm and 7.7 mm in diameter (Ryerson, 1995; Veron, 2015). Smaller droplets with low *St* remain entrained in the airstream, and if a spray-flux measuring device is able to capture these smaller droplets, it is more likely to collect larger droplets with higher *St*, as higher *St* values result in increased collision efficiency due to greater body force (Lennox et al., 2013). Here, collision efficiency refers to the fraction of liquid water in the volume swept out by an object that actually collides with its surface (Finstad et al., 1988).

Therefore, the qualitative performance of the spray-flux measuring device can be assessed by analysing the wind flow around it, which provides insight regarding the collection efficiency. In this context, collection efficiency refers to the ratio between the number or mass of droplets successfully collected or accounted for by the device and the total number of droplets in the sampled air stream (Montecinos et al., 2018). In this study, steady-state wind flow simulation using the RANS k-ω SST turbulence model (Menter et al., 2003; Menter, 1994) is utilised, as the information on time-averaged velocity and turbulent fluctuations to evaluate the performance of the device is found sufficient.

3.2. Boundary condition and discretisation

The computational domain for the wind tunnel simulation was a 3 m × 2 m × 2 m rectangular box that represents the environment (Fig. 11). The model of the spray measuring device being studied is located in the centre of the box. The x-axis runs along the width, the y-axis is the vertical direction, and the z-axis is the longitudinal direction. The origin point of these axes is at the base of the model, specifically in the centre of their cross-section. The domain is described using an unstructured mesh that combines tetrahedral and/or prismatic elements, which is determined by the specific geometries used in the simulation. Table 3 provides the list of the parameters used in the simulations.

Mesh convergence analyses were performed for each device simulation, affirming that the mesh utilised was sufficiently refined, with additional refinement yielding no significant impact on simulation results. The total number of elements in mesh on convergence and used in the simulation is listed in the Appendix, Section A.1, Table A.1.

4. Analysis of the sea-spray flux measuring devices

This section presents an analysis of the sea-spray flux measuring devices used in field expeditions, supported by the CFD simulations, following the methodology outlined in Section 3.2. The objective is to assess the performance and efficiency of the devices in collecting sea spray by studying airflow patterns, as described in Section 3.1. The analysis of each device is divided into two parts: one focusing on the sea-spray collector design and issues and the other on the method of quantifying the collected spray amount. For reference, the dimensions of the CAD models employed in the CFD simulations within this section are provided in Appendix Section A.1, Table A.1.

4.1. Sea spray collector device consisting of absorption cylinder and wind cups

4.1.1. Collector design analysis

The simulation (Fig. 12) of wind flow around Tabata's (1969) device shows that when the cylinder is placed in airflow, flow separation occurs, causing the airflow to detach from the cylinder surface and form a turbulent wake behind it (Houghton et al., 2017). This separation reduces the collision efficiency as this phenomenon takes place on the windward side of the cylinder, particularly for smaller droplets with low Stokes numbers that follow the airflow around the cylinder without effective collisions. Moreover, in the case of this device with a rotating cylinder made of absorbent material (toilet paper), not all the colliding spray droplets are absorbed; some may bounce off.

The rotation of the cylinder causes uneven pressure symmetry, affecting the airflow around the surface. The Coanda effect further influences the flow pattern by causing the airflow to adhere to the curved surface of the cylinder (Panitz and Wasan, 1972). Initially, as the cylinder starts to rotate, the absorbing efficiency (i.e., here, absorbing efficiency is defined as the ratio of the absorbed droplet mass flux to the impinging droplet mass flux) increases due to the larger surface area of the absorbent paper exposed to wind. However, the efficiency may decrease with faster rotation at higher wind speeds as droplets have less time to collide and be absorbed before being flung off the cylinder. Additionally, the absorbing capacity is influenced by exposure time, and absorbent materials like toilet paper may become saturated over time. Consequently, using this setup in areas with high spray flux and heavy weather conditions is not practical, as the absorbent material may saturate quickly, leading to measurement errors.

4.1.2. Measurement method analysis

According to Tabata (1969), the toilet paper rolls had to be replaced every five to six minutes during spray events, and the soaked rolls were placed in a polyethene bag and weighed upon arrival at the port. Any account for the consideration of the evaporated amount is not mentioned.

4.2. Drums

4.2.1. Collector design analysis

The wind flow simulation around the drums used for spray distribution measurement on Tarsiut Island (Muzik and Kirby, 1992) demonstrates that the collection efficiency of the gauge decreases with increasing wind speed. This is attributed to the pressure bias (Fig. 13 (a)) near the drum orifice, which can cause spray droplets to miss or be deflected away from the orifice (Fig. 13 (b) and 12 (c)). Consequently, the measured spray amount is underestimated. This is a prevalent error associated with catching-type precipitation gauges due to their physical shape, referred to as "wind-induced undercatch" (Pollock et al., 2018). Winds higher than 15–20 m/s can significantly decrease the amount of precipitation caught by such gauge, often by up to 50% (Ryerson and Longo, 1992). Furthermore, the data collected with this method only considers the vertical spray flux that falls directly onto the drums (Mintu and Molyneux, 2022), which does not account for the spray flux in the horizontal direction.

Table 4
Summary of the sea-spray field measurements.

Measurement period	Measurement site	Region	Device / method used	Spray parameters measured	Reference
1963–1967	12 Japanese Patrol boats (270-ton - 1100-ton class)	Nearby Hokkaido, Primorsky Krai, the Kuril Islands, and the Kamchatka region	Visual	Spray amount	Tabata (1969)
28–30 July 1964	Patrol boat Chitose (350- ton class)	Outside Wakkanai Port, Japan	Sea-spray collector consisting of water absorbing cylinder made of toilet paper roll and wind cups	Spray flux	
February 1968	MFV Academic Ber (39.5 m long)	Sea of Japan	Visual´	Spray frequency	Golub'iev (1972); Gurvitch (1972); Panov (1976) *
March 1968	MFT Aland (54.2 m long)	Barents Sea	Visual´	Spray frequency	Aksyutin (1979); Gurvitch (1972); Rozenberg (1971)*
March 1968	Siener Murmanchanin	Bering Sea´	Visual´	Splashing of the ship with spray	Rozenberg (1971)*
April 1968	MFV Academic Knipovitch	Barents Sea	Visual´	Spray frequency	Rozenberg (1971)*
April 1968	MFV Polyarnik (38.5 m long)	Barents Sea	Visual´	Splashing the ship with spray	Gurvitch (1972; Rozenberg (1971)*
January – February 1969	MFV Academic Ber (39.5 m long)	Sea of Japan	Visual´	Spray frequency	Panov, (1976) *
January – February 1969	MFV Professor Somov (39.2 m long)	Barents Sea	Visual´	Splashing of the ship with spray	Gurvitch (1972; Rozenberg (1971)*
August – November 1969	MFV Iceberg (39.2 m long)	North Atlantic Ocean	Unknown	Droplet size LWC on different locations (horizontal and vertical surfaces)	Gashin's work published in Borisenkov (1972); Borisenkov and Panov (1972)
			Unknown	Spray duration	
February 1973	MFV Narva (39.5 m long)	Sea of Japan	Droplet size measured by trapping droplet in a mixture of soot and viscous oil (1:3 ratio) deposited on a metal substrate. Also, an absorbent and colouring substrate.	Droplet size (wind and collision generated spray)	Borisenkov et al. (1975); Panov (1976)
			Specially designed traps (unknown construction) by the Leningrad Polytechnic Institute	LWC (vertical profile)	
			High-speed camera	Spray duration	
unknown	Ship (unknown)	unknown	10–20 mm oil-coated glass slides attached to a boom extending from a ship at 1.5–2, 4, and 7 m above the sea surface	Droplet size (wind-generated spray)	Preobrazhenskii (1973)
19–20 July; 20–21 August; 6–8 September; 17 September	Tarsiut Island	Beaufort Sea	Spray collected in 45-gal drums (0.56 m diameter by 0.8 m high)	Spray flux distribution on the island	Muzik and Kirby (1992)
April 1983 – December 1984	Semi-submersible drilling rig Treasure Scout	Barents Sea	Absorbent panels made with baby diaper	Vertical spray flux distribution	Jorgensen, (1986, 1985, 1984)
			Pipe bend collector	Horizontal spray flux distribution	
			High-speed camera	Droplet size	
			Visual	Spray frequency	
September 1985 – January 1986	Jacket platform Edda	North Sea	Absorbent panels Pipe bend collector	Limited measurements collected due to safety concerns during high winds	
5–6 October 1985, 18–19 December 1985, and 21–25 January 1986	Sister ships Tender Turbot and Tender Trout	Central North Sea region	Pipe bend collector	Horizontal spray flux distribution	Horjen et al. (1986)
			Visual	Spray frequency	
5 September – 25 November 1985	Stand-by vessel Endre Dyrøy	Central Bank (74°30′ N, 31°00′ E)	Pipe bend collector	Horizontal spray flux distribution	
5–9 April 1986	Supply ships Troms Tjeld	southwestern Barents Sea	Pipe bend collector	Horizontal spray flux distribution	
			Visual	Spray frequency	
5 February – 13 March 1990	USCGC Midgett (115 m long)	Gulf of Alaska and the Bering Sea	Horizontal spray interceptor	Horizontal spray flux distribution	Ryerson and Longo (1992); Ryerson (1995)
			Vertical spray collector	Vertical spray flux distribution	
			Young automatic rain gauges (Model 50,202)	Vertical spray flux distribution	
			Rain and snow gauges (Model 6310-A)	Vertical spray flux	
			Video camera	Estimate the duration and characteristics of spray events	

(*continued on next page*)

Table 4 (*continued*)

Measurement period	Measurement site	Region	Device / method used	Spray parameters measured	Reference
			Universal flying particle camera	Droplet size	
1990	USCGC Midgett (115 m long)	Bering Sea	Ship Motion Recorder (SMR) and a tri-axial accelerometer	Ship motion	Thomas (1991)
			Video cameras	Spray events	
1991	USS Monterey (173 m long)	northwest North Atlantic Ocean	Ship Motion Recorder (SMR) and a tri-axial accelerometer	Ship motion	
			Video cameras	Spray events	
December 2012 – January 2013	Mt. Desert Rock	Gulf of Maine, 38 km south of Bar Harbor	Microscope slides coated with Vaseline	Droplet size (wind-generated spray)	Jones and Andreas (2013); Andreas (2016); Jones and Andreas (2014)
			CIP	Droplet size and near-surface spray concentration	
January – February 2014	Mt. Desert Rock	Gulf of Maine, 38 km south of Bar Harbor	Rotating multicylinder covered with absorbent paper and microscope slides	Characterize droplet size distributions (wind-generated spray)	
July – August 2012	CCGS Icebreaker Louis S. *St*-Laurent (11,345 GT)	*St.* John's to Lancaster Sound and Canada Basin	SPC	Droplet size distribution and volume flux	Ozeki and Sagawa, (2013); Shiga et al. (2015); Ozeki et al. (2016, 2018); Ozeki et al., (2016b)
2013–2014 (JARE-55) and 2014–2015 (JARE- 56)	Icebreaker Shirase (12,650 GT)	Antarctic Ocean region	SPC	Droplet size distribution and volume flux	
			MRS	Volume flux distribution	
22 August – 2 October 2016 (ArCS 2016)	R/V Mirai (8706 GT)	Arctic Ocean, Bering Sea, and North Pacific region	SPC and MRS	Droplet size and volume flux vertical distribution	Ozeki et al. (2016c); Fushimi et al. (2019); ArCS (2016, 2018, 2019, 2021)(Ozeki et al. (2016b)
24 October – 7 December 2018 (ArCS 2018)	R/V Mirai (8706 GT)	Arctic Ocean, Bering Sea, and North Pacific region	SPC and MRS	Droplet size and volume flux distribution	
27 September – 7 November 2019 (ArCS 2019)	R/V Mirai (8706 GT)	Arctic Ocean, Bering Sea, and North Pacific region	SPC and MRS	Droplet size and volume flux distribution	
11 September – 17 October 2021 (ArCS 2021)	R/V Mirai (8706 GT)	Arctic Ocean, Bering Sea, and North Pacific region	MRS	Volume flux in the bow region	
winter seasons of 2017–2018 and 2018–2019	Norne FPSO	Norwegian Sea	Rigspray Fluxmeter Video recording system	Spray flux Bow spray events	Teigen et al., (2019)

MFV - Medium-sized fishing vessel, MFT - Medium-sized freezing trawler, FPSO - Floating production, storage and offloading, GT – Gross Tonnage.
* Information found from Zakrzewski and Lozowski (1989); ´Most Likely.

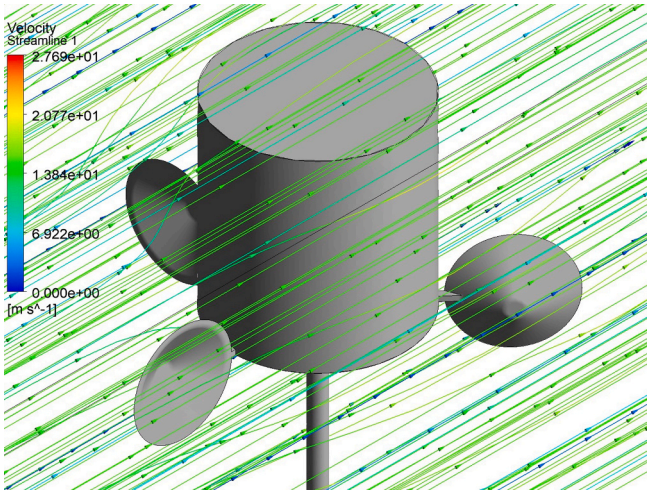

Fig. 12. The CFD simulation (15 m/s) of the wind flow of the sea-spray collector device used by Tabata (1969).

4.2.2. Measurement method analysis

Muzik and Kirby, 1992 reported that the collected spray level was manually recorded during strong weather events at regular intervals, and there was no mention of an automatic measuring system. However, the manual approach poses safety risks for personnel carrying measurements in rough weather conditions and may introduce potential errors, such as those arising from sloshing due to liquid movement within the container and parallax resulting from viewing angle discrepancies.

4.3. Absorbent panels

4.3.1. Collector design analysis

According to the simulations, the absorbent panel (made with baby diaper (Jorgensen, 1984)) shape causes flow separation (Fig. 14 (a) and 14 (b)) due to a pressure bias, with higher pressure on the front than the backside. As a result, the collision efficiency decreases as wind speed increases, reducing contact between spray droplets and the absorbent material. Turbulent conditions can further diminish the absorbing efficiency, as droplets may be carried away before being absorbed. Moreover, the absorbent capacity of the material diminishes over time. Consequently, using this setup in high spray flux and adverse weather conditions may introduce measurement inaccuracies.

4.3.2. Measurement method analysis

The soaked absorbent panels were weighed using a spring balance to measure the vertical spray flux. However, this method may introduce errors because of the acceleration of the moving platform.

4.4. Bend pipe collector

4.4.1. Collector design analysis

The simulation around the bend pipe collector indicates that when the air-borne droplets are carried at higher wind velocity can lead to the

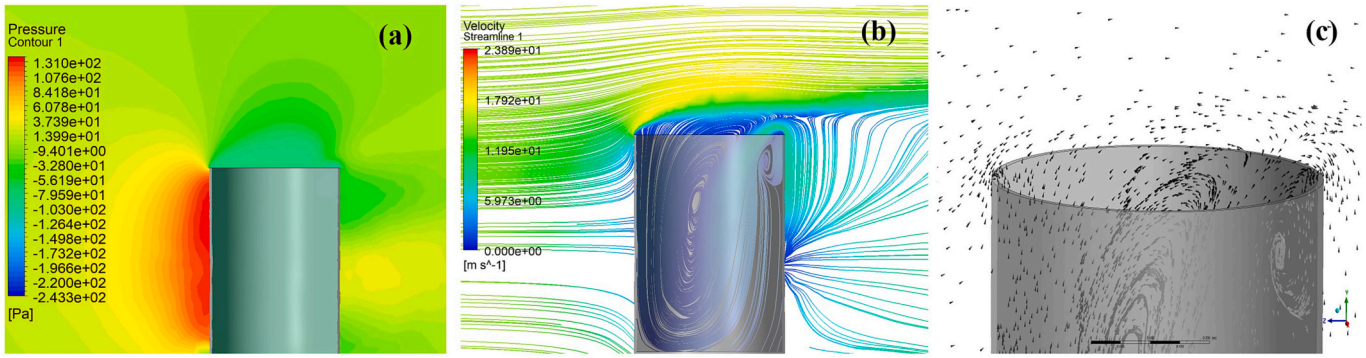

Fig. 13. (a) The CFD simulation (15 m/s) shows the pressure field around the drum; (b) wind flow field around the drum; (c) flow field around the orifice.

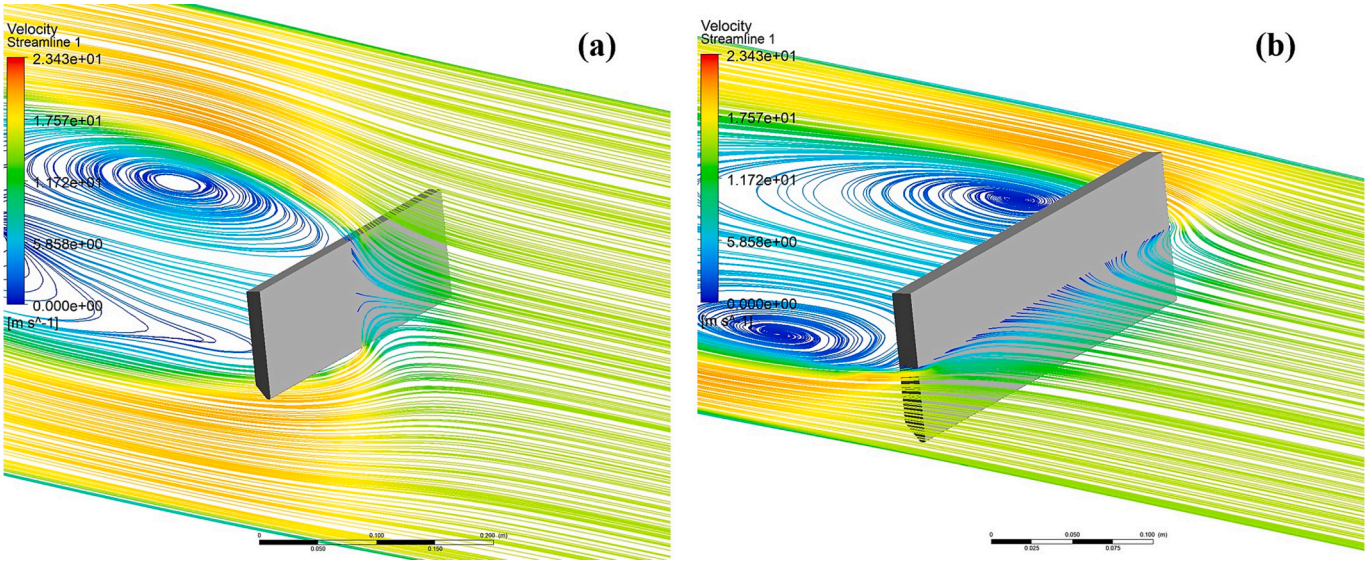

Fig. 14. (a) The CFD simulation (15 m/s) shows the wind field in a vertical plane; (b) Wind field in a horizontal plane (both planes crossing the centre of the absorbent panel).

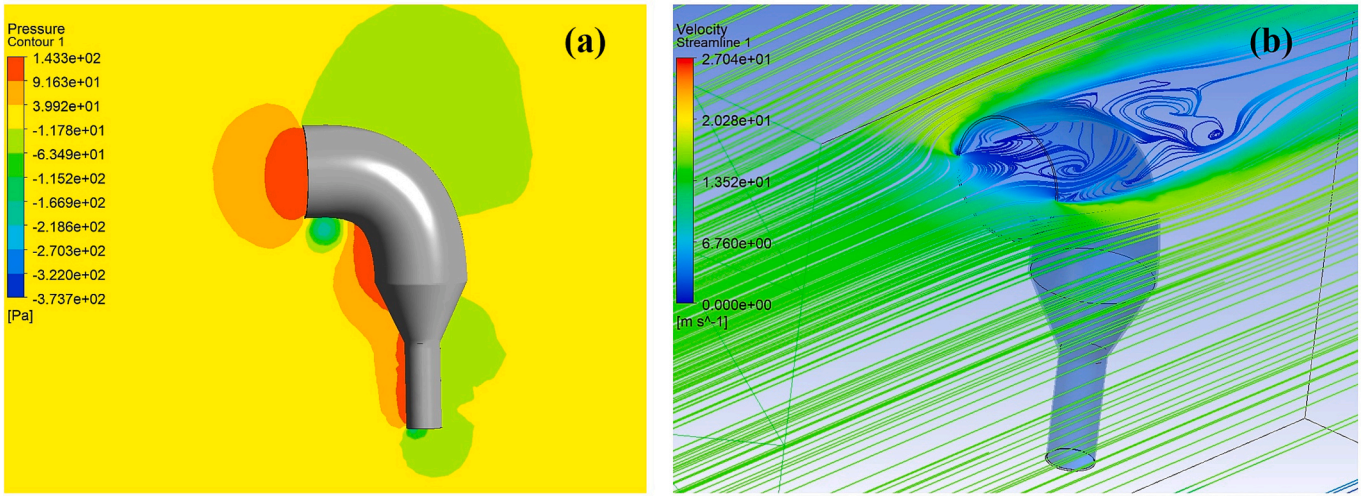

Fig. 15. (a) The CFD simulation (15 m/s) shows the pressure field across the bend pipe collector; (b) the wind flow around the bend pipe collector.

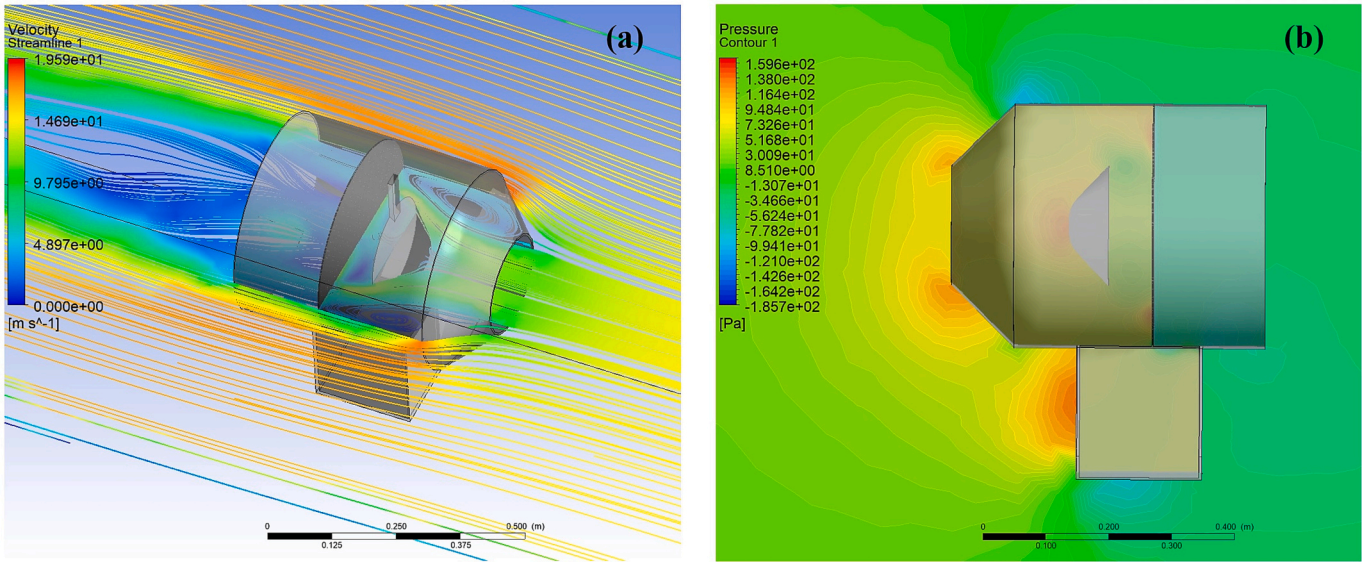

Fig. 16. (a) The CFD simulation (15 m/s) shows the wind flow around the CRREL horizontal spray interceptor; (b) pressure field across the horizontal spray interceptor.

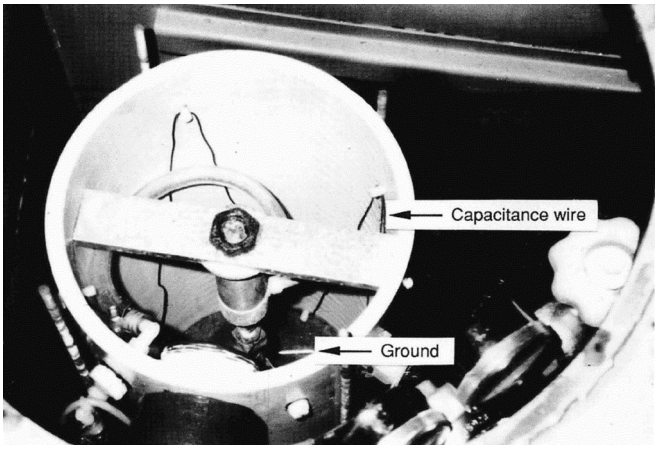

Fig. 17. Capacitance wire measurement system in the tank.

formation of an air plug at the inlet. This is caused due to the pressure bulb located around the opening, as depicted in Fig. 15 (a), which blocks the airflow due to the dead-ended or constricted design of the collector. As the wind speed increases, the pressure bulb intensifies, resulting in most spray droplets not entering the collector but instead passing around the bulb (evident in Fig. 15 (b)). The air plug may significantly reduce the collection efficiency. Only larger droplets with higher kinetic energy and momentum may have the ability to overcome the resistance created by the pressure bulb and enter the collector. The larger droplets with higher stokes numbers possess more body force which helps them to resist airflow deviation.

4.4.2. Measurement method analysis

During the field expedition, manual readings were taken from the level gauge attached to the pipe bend collector. However, this approach poses risks in adverse weather conditions and difficulty accessing equipment (Horjen et al., 1986). Additionally, parallax errors may occur when reading the spray level.

4.5. CRREL horizontal spray interceptor

4.5.1. Collector design analysis

The wind simulation of the CRREL horizontal spray interceptor (Walsh et al., 1992) demonstrates effective airflow dynamics. The air enters the constricted inlet, flows through the large internal chamber with twice the inlet diameter, then flows around the convex baffle and exits through the mesh at the back (Fig. 16 (a)). The design utilises the Venturi effect (Venturi, 1797), which minimises flow separation and prevents the formation of a pressure bulb at the inlet (Fig. 16 (b)). This results in enhanced airflow and efficient transport of spray droplets within the collector.

4.5.2. Measurement method analysis

A system with Teflon-coated capacitive wire (Fig. 17) was designed to measure the spray level automatically in the collecting tank. However, the system produced fluctuating and noisy measurements during the Midgett expedition. The noise in the spray data was attributed to the measurement of saline spray instead of fresh water (Ryerson and Longo, 1992). There were only minimal noise issues before filling the tanks with seawater and draining them for the first time. The noise significantly increased after the capacitive wires became covered with saltwater. Variations in the wetness of the wires due to splashing and humidity changes likely contributed to the noise problem.

4.6. CRREL vertical spray collector

4.6.1. Collector design analysis

A rain gauge-like collector with a 30 cm diameter funnel was used to measure vertical spray flux (Walsh et al., 1992). Similar to the drum simulation discussed in Section 4.2, this collector faced the problem of undercatch (Ryerson and Longo, 1992).

4.6.2. Measurement method analysis

The CRREL vertical collector collected spray in the measuring tank with the same capacitive wire system as for the horizontal collector (Section 4.5). However, the noise in the vertical spray flux collectors was noticeably lesser. This suggests the presence of an additional factor

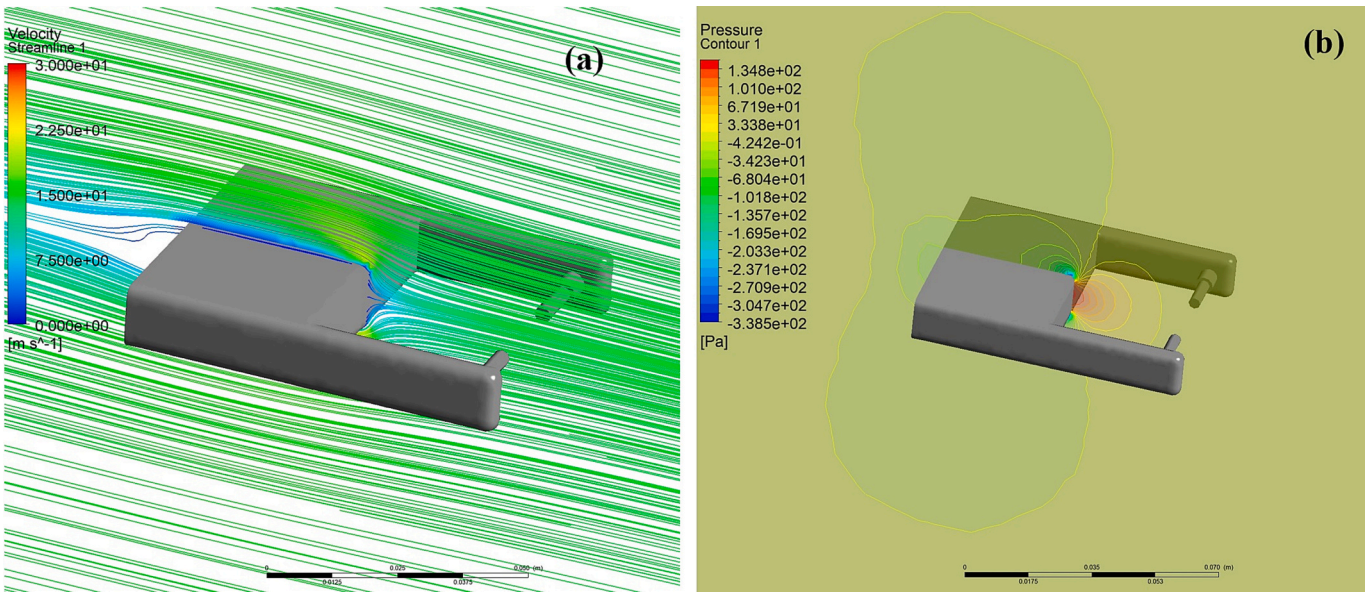

Fig. 18. (a) The CFD simulation (15 m/s) showing the wind flow across the SPC sensor; (b) pressure field across the SPC sensor.

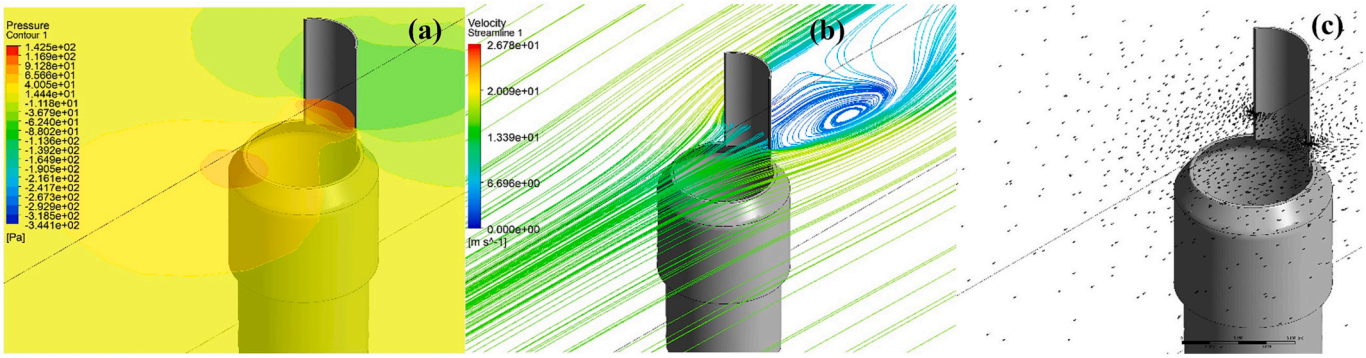

Fig. 19. (a) The CFD simulation (15 m/s) of MRS showing the pressure field around spray trap mounted on top of the Young gauge (Model 50,202); (b) flow field around the around the spray trap; (c) wind flow around the spray trap.

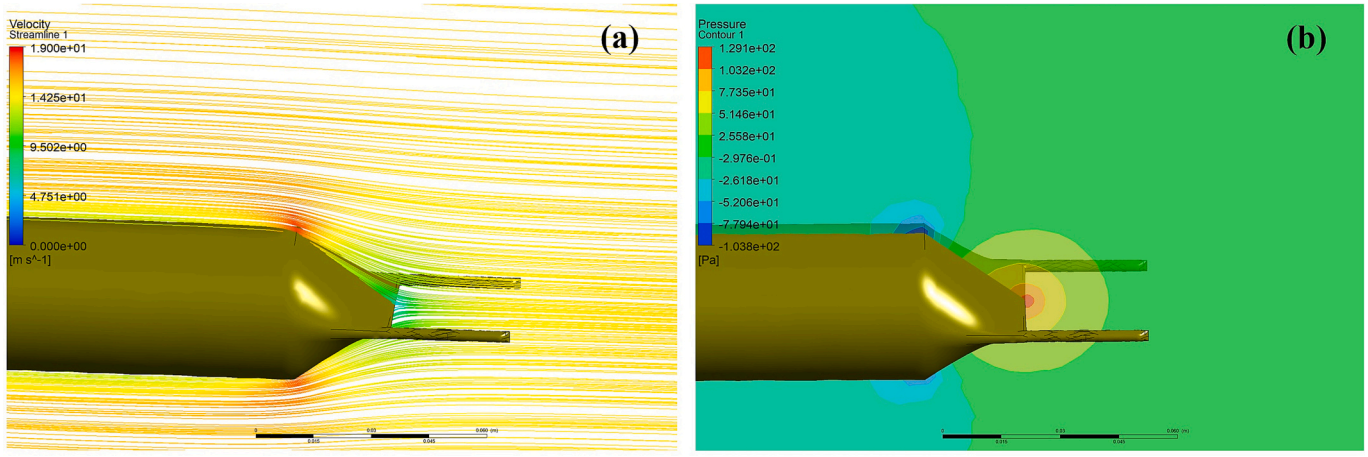

Fig. 20. (a) The CFD simulation (15 m/s) shows the wind flow across the CIP (Cloud Imaging Probe) sensor; (b) pressure field across the CIP sensor.

amplifying the noise, possibly related to the horizontal collectors (Ryerson and Longo, 1992). The increased noise in the horizontal collector is believed to be due to its higher filling and draining frequency (as they intercepted more spray), the fast-moving air passing through the collectors causing splashing in the tank water, and the quick changes in humidity resulting from the scooping action of the collectors, which may have contributed to the noise.

4.7. Spray particle counter

4.7.1. Design analysis

The Spray Particle Counter (SPC) (Ozeki et al., 2016b) is an optical measuring device designed with an aerodynamic shape that minimises drag and allows the sensor probe to move through the air with minimal resistance as long as it is oriented towards the wind. The body shape is intended to promote smooth airflow and reduce turbulence to avoid flow separation (see Fig. 18 (a) and (b)). The protruding sensor component is positioned such that it can account for the droplets whose trajectories are uninterrupted. This maximises the number of droplets that pass through the sensor, thereby increasing the chances of successful measurements and accurate data collection.

4.7.2. Measurement method analysis

The device can count droplet sizes ranging from diameter 100–1000 μm and accordingly is divided into 32 bins by the processor. The measuring frequency is 1 Hz. The volume flux of the spray is estimated by the formula of sphere volume $4\pi r_c^3/3$, where r_c is the class value of droplet radius. The volume flux unit is the same as precipitation which is mm per unit of time.

4.8. Marine rain gauge type Spray gauge

4.8.1. Design analysis

The airflow simulation around the marine rain gauge type spray gauge (MRS) spray trap (Ozeki et al., 2016b) shows that pressure bias causes flow separation (Fig. 19 (a)), deflecting the airstream away from the trap (Fig. 19 (b) and Fig. 19 (c)). This leads to smaller droplets bypassing the trap, while only larger droplets collide with the trap. As wind speed increases, this becomes more prominent, as even larger droplets that could potentially collide with the trap may bounce and be carried away by the wind. Consequently, the spray fails to enter the gauge, reducing the MRS collection efficiency. The small size of the spray trap may also limit its ability to block high spray volume, potentially resulting in missed measurements.

4.8.2. Measurement method analysis

The spray amount collected in the MRS is automatically measured with the R.M. Young rain gauge (Model 50,202). The device uses a capacitive sensor around a measuring tube to determine the water level. It has no moving parts, making it suitable for use on moving platforms, such as ships and floating buoys (Weller, 2018). The readings can be recorded using a data logger for continuous autonomous measurements. Once the device is filled, it self-siphons the water, starting another measurement cycle.

4.9. Cloud-imaging probe

4.9.1. Design analysis

The simulation shows that the streamlined cylindrical body of the cloud-imaging probe (CIP) (Andreas, 2016) minimises drag and allows smooth airflow when facing the wind (Fig. 20 (a) and (b)). The extended sensor probes aligned towards the wind account for spray droplets unaffected by flow separation, ensuring accurate measurements.

4.9.2. Measurement method analysis

The CIP can detect spray droplets and measure their sizes as they pass through its probe within its measurement range (6.25–775 μm radii for the model used by Andreas (2016)). It also provides the LWC, which can be used to calculate the spray flux.

4.10. RigSpray fluxmeter

4.10.1. Collector design analysis

The CFD simulation of the Fluxmeter collector plate (Teigen et al., 2019) illustrates the influence of airflow on sea spray droplet trajectory (see Fig. 21 (a) and 21 (b)). The plate placed in an airflow creates a high-pressure zone in the front and a low-pressure zone behind (Fig. 21 (c)), resulting in vortexes. This diverts the airflow around the plate, causing smaller droplets to be carried away and reducing their collision with the plate. Heavier droplets are more likely to collide and collect in the instrument cabinet for measurement. The design of the collector plate resembles a vertical surface, such as the bulkhead of a marine structure, to measure spray flux impinging on such surfaces. As wind speed increases, the stronger pressure bias makes it more challenging for spray droplets to land on the plate, further reducing collision efficiency.

4.10.2. Measurement method analysis

The spray intercepted by the plate is directed into the instrument cabinet through a pipe and collected in a tipping bucket. A pressure gauge is integrated into the bucket to measure the water level by detecting the corresponding pressure change during the collection process.

5. Discussion

The performance of spray measuring devices can be discussed from the perspective of the effectiveness of the methods used to measure important sea spray parameters, including LWC, spray frequency, duration, and droplet size distribution. Furthermore, evaluation of the practicality in operational settings should consider various components of the devices, emphasising the collector part design, spray amount measurement part, and logging aspects. By integrating the performance of both measurement methods and device components, valuable insights

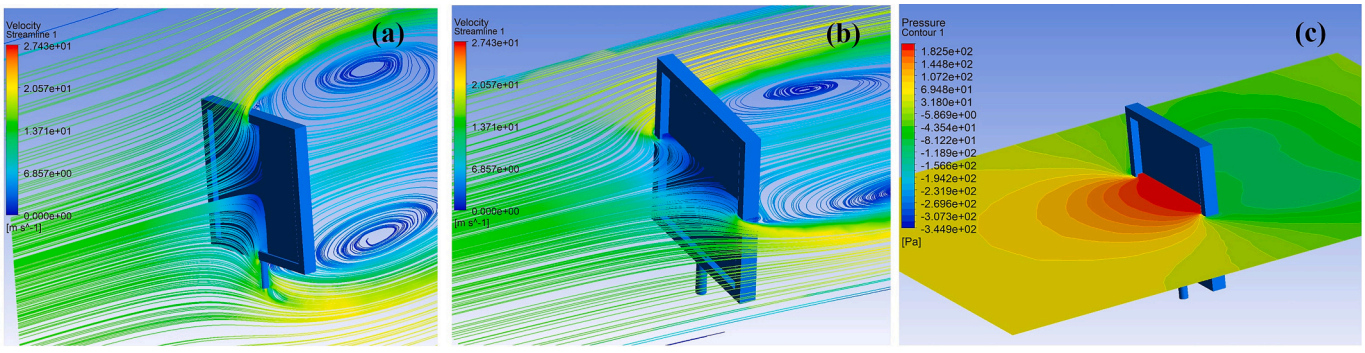

Fig. 21. (a) The CFD simulation (15 m/s) shows the wind field in a vertical plane. (b) wind field in a horizontal plane (both planes crossing the centre of the collector plate of the RigSpray Fluxmeter). (c) pressure field in a horizontal plane.

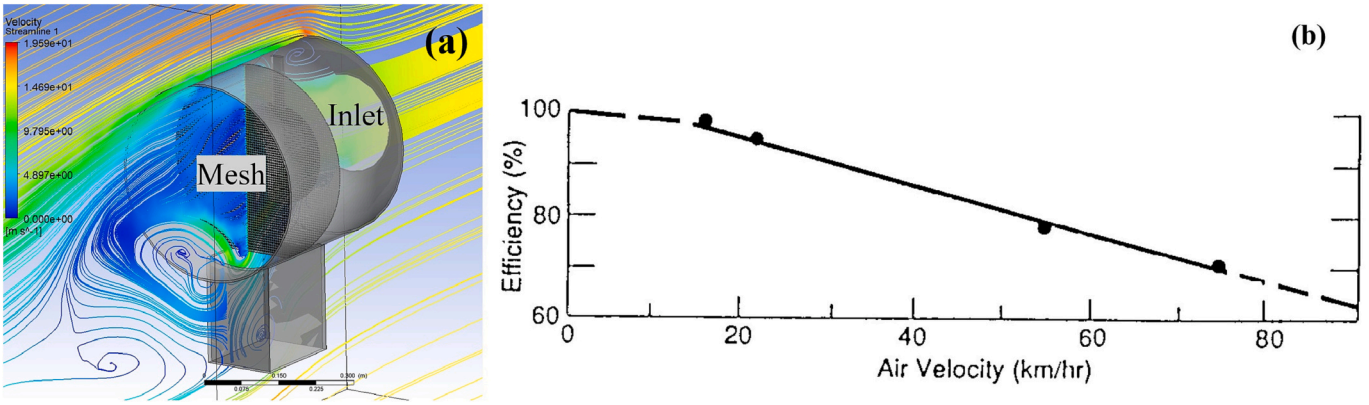

Fig. 22. (a) The CFD simulation (15 m/s) showing the wind flow from the mesh screen of the CRREL horizontal spray interceptor. (b) Efficiency curve for calibration of the horizontal spray interceptor (Walsh et al., 1992).

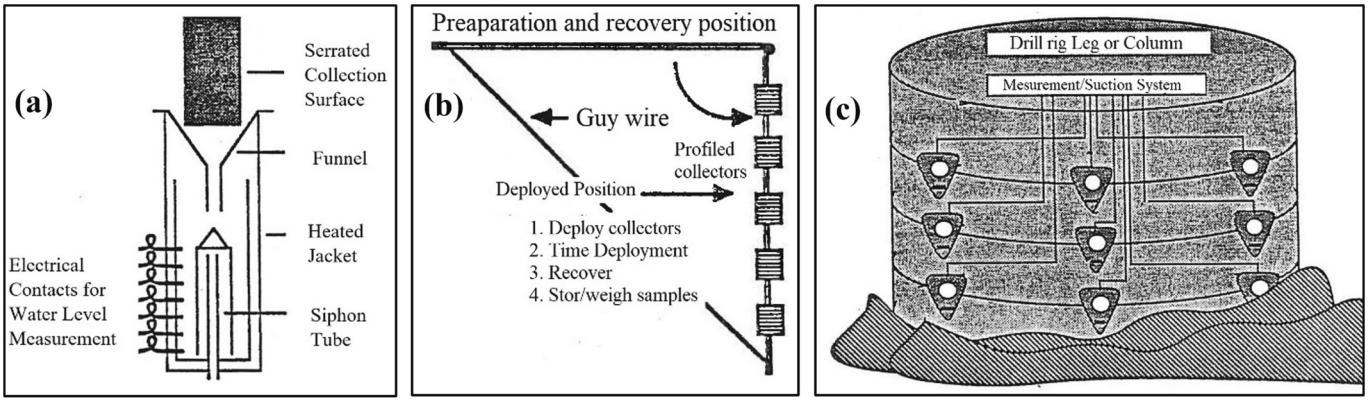

Fig. 23. (a) Water level measurement system prototype (1987); (b) a sea spray "profiling system"; (c) measurement system on a rig column (Roebber and Mitten, 1987).

are gained, enabling the identification of strengths, limitations, and potential areas for improvement in the measurement methods and device components.

The devices used to measure droplet sizes, such as high-speed cameras, SPC (Ozeki et al., 2016c), and CIP (Andreas, 2016), are suitable for remote data collection with minimal assistance. However, it is important to consider that these devices are designed to measure droplet sizes within specific ranges. As sea spray droplet sizes can vary significantly, ranging from 0.02 μm to 7.7 mm in diameter (Ryerson, 1995; Veron, 2015), one specific device might not cover the entire spectrum. Additionally, it should be acknowledged that these techniques provide measurements of a small sample volume, which may not be representative of the droplet size distribution of the entire spray cloud.

Spray frequency data is primarily collected through visual counting, which has limitations regarding the quantity of data that could be collected and the accuracy due to subjective assessment. For instance, Jorgensen (1984) reported a discrepancy of approximately 10% in spray frequency measurements counted by two observers. Regarding the spray duration measurement, during the Midgett expedition, spray duration data were obtained from 39 events by meticulously analysing camera footage frame by frame (Ryerson, 1995). Acquiring spray frequency and duration data through these techniques is time-consuming and cumbersome, leading to limited available data.

The sea-spray flux measuring devices utilising absorbent materials like toilet paper (Tabata, 1969) and baby diapers (Jorgensen, 1984) are inexpensive but prone to saturation and unsuitable for autonomous measurement. Optical instruments like SPC (Ozeki et al., 2016c) and CIP (Andreas, 2016), despite their aerodynamic shapes and ability to account for horizontal and vertical flux, have limited droplet size measurement capabilities. They are costly, delicate, and may need frequent maintenance when deployed in saline marine environments.

Catching-type collector designs like drums (Muzik and Kirby, 1992), bend pipe collector (Horjen et al., 1986; Jorgensen, 1984), CRREL horizontal and vertical spray collector (Ryerson and Longo, 1992), MRS (Ozeki et al., 2016c), and RigSpray Fluxmeter (Teigen et al., 2019) are favoured for their ease of manufacturing and long-term deployment in harsh weather conditions. However, they face problems related to flow separation due to their bluff body shape, leading to decreased collection efficiency. Quantifying the wind-induced measurement error is essential to avoid establishing all modelling and subsequent decision-making based on flawed knowledge (Colli et al., 2018). There are experimental (Pollock et al., 2018; Cauteruccio et al., 2021) and numerical methods (Colli and Lanza, 2016; Colli et al., 2018) used to address this issue. Windshields can be employed for vertical collectors to minimise wind-induced undercatch (Colli et al., 2016).

Among the horizontal collector designs, the CRREL horizontal spray interceptor (Walsh et al., 1992) has an efficient design to keep the flow separation minimal. However, with an increase in wind speed, its collection efficiency decreases, as smaller droplets entrained in the airflow may escape through the mesh at the back of the collector instead of falling into the measurement tank (Fig. 22 (a)). Walsh et al. (1992) presented a calibration curve (Fig. 22 (b)) based on experimental results to compensate for this efficiency decrease. However, it only accounts for droplets of diameter 0.5 mm, while real-world scenarios may involve

even smaller sea spray droplets, which further reduces the efficiency. Additionally, some smaller droplets may not enter the collector due to pressure perturbations at the inlet, which are also not accounted for in the experimental efficiency graph.

An automatic measuring device is the preferred method for logging the amount of collected spray due to the various advantages it offers. Notably, it provides larger amounts of data over extended periods, which can be beneficial in more advanced data analysis methods, including those based on machine learning. Moreover, it eliminates the need for constant human presence during harsh weather conditions, leading to enhanced safety in data collection campaigns.

The automatic capacitive water level measuring system (Walsh et al., 1992) used in the Midgett expedition exhibited high noise. Ryerson and Longo (1992) evaluated various methods and found that tipping and weighing buckets were unreliable due to the potential errors caused by ship motion. Instead, buckets (with float) or capacitive sensors in stilling wells and ultrasonic level detectors were identified as suitable alternatives. The RigSpray Fluxmeter (Teigen et al., 2019) design employs a tipping bucket arrangement, which also may be influenced by platform movement. The R.M. Young rain gauge (Model 50,202) performed well during the Midgett expedition (Ryerson and Longo, 1992) and during its use in MRS (Ozeki, personal communication, 2022). The gauge reading is also unaffected by the moving platform, making it a reliable choice.

Roebber and Mitten's (1987) report provides guidance on planning field expeditions, which includes suggestions on equipment for collecting sea-spray data. An illustration of a measurement system for collecting and measuring spray is presented (Fig. 23 (a)). The system was developed at the National Research Council Canada. It included a serrated surface, funnel, electrical contacts, and a heated jacket and utilised a siphon tube or an electrical dump valve for draining (described by Stallabrass in personal communication with Roebber and Mitten). Another option suggested is a sea spray "profiling system" (Fig. 23 (b)) with collectors at different heights on a pole. Zakrzewski proposed (personal communication with Roebber and Mitten) placing collectors below the main deck of a rig to capture spray from different directions and heights (Fig. 23 (c)). Each collector would have an evaporation barrier, an electrically controlled suction, measurement, and a draining system for automated operation.

Ryerson and Longo (1992) proposed some optical-based measurement systems, concerning the equipment malfunctioning issues they encountered. They recommend particulate volume counters, such as Laser Doppler Velocimeter and Particle Analyser, as potential options to measure sea spray, as they have the ability to detect small changes in spray flux. The optical instruments offer the advantage of directly measuring local LWC without significantly disturbing the surrounding wind field. The spray mass flux at the icing location is proportional to the droplet impact velocity and will hence depend more on test conditions. More recently, Dhar (2021) and Dhar and Khawaja (2021) proposed how LiDAR equipment might benefit sea spray measurement because of its high spatial and temporal resolution.

6. Concluding remarks

In this critical review, various techniques and devices used in field expeditions for collecting sea spray data are analysed. CFD simulations are utilised in order to assess the efficiency of spray flux measuring devices. The review also provides a summary of the field expeditions that were carried out with the objective of collecting data on spray characteristics, including liquid water content, spray frequency, duration, and droplet size distribution. These parameters are crucial for developing robust spray-flux expressions, which is a key part of accurate marine icing estimation.

Visual counting, commonly used for spray frequency data, has limitations in terms of data quantity and accuracy due to subjective assessment. Frame-by-frame analysis of video footage for spray duration is time-consuming and yields limited data. Therefore, there is a need for more efficient techniques, potentially incorporating machine learning algorithms for automated spray event counting and duration estimation from video recordings.

Absorbent material-based sea-spray flux measuring devices offer cost-effective solutions but are prone to saturation and require regular replacement and weighing. Optical instruments have advantageous designs but limited capabilities in measuring a wide range of droplet sizes. They are also costly and may require frequent maintenance in marine environments.

Catching-type collector designs are favoured due to their ease of manufacturing and suitability for long-term deployment in harsh weather conditions. However, the flow separation issue leading to decreased collection efficiency needs to be addressed. Quantifying wind-induced measurement errors is crucial for improving their accuracy. Our CFD simulations demonstrated that the CRREL horizontal spray interceptor has an efficient design compared to other horizontal catching-type collectors. However, its collection efficiency decreases at higher wind speeds, highlighting the need to overcome this limitation.

For logging the amount of collected sea spray, automatic measuring devices are ideal. These devices continuously log the collected spray level and automatically empty when full, ensuring uninterrupted autonomous measurements. The R.M. Young automatic rain gauge (Model 50,202) has demonstrated satisfactory performance in prior field expeditions and is suitable for installation on moving platforms, making it a viable option.

In conclusion, this critical review provides valuable insights into the advantages and limitations of techniques and instruments used in sea-spray data collection. We emphasise the importance of selecting appropriate measurement systems tailored to the challenges, which will contribute to the development of robust marine icing models. While standard equipment or methods for such measurements are currently unavailable, researchers have employed diverse equipment designs based on their specific requirements. By identifying areas for improvement and considering insights gained from CFD simulations, future researchers can design more efficient systems for comprehensive and reliable sea-spray data collection.

Declaration of generative AI and AI-assisted technologies in the writing process

During the preparation of this work, the author(s) used ChatGPT in order to improve readability and language. After using this tool/service, the author(s) reviewed and edited the content as needed and take(s) full responsibility for the content of the publication.

Declaration of Competing Interest

The authors declare that they have no known competing financial interests or personal relationships that could have appeared to influence the work reported in this paper.

Data availability

No data was used for the research described in the article.

Acknowledgements

We would like to thank the Research Council of Norway for their financial support through the project "Multidisciplinary approach for spray icing modelling and decision support in the Norwegian maritime sector" (SPRICE) funded under MAROFF-2 Programme [Grant Number: 320843]. We would also like to extend our sincere appreciation to Dr. Toshihiro Ozeki for the insightful personal communication and for generously sharing valuable information regarding their work.

Appendix A. Appendix

Table A.1. CAD model dimensions and total number of mesh elements used in the CFD simulations.

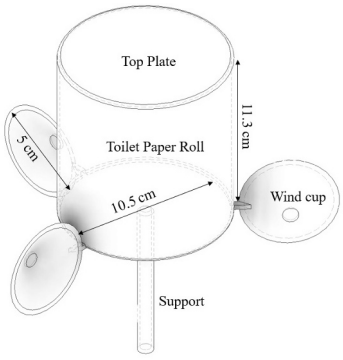

Fig.A.1. Model used in Section 4.1.
Number of elements: 3,380,452

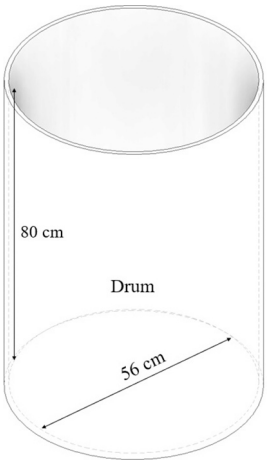

Fig.A.2. Model used in Section 4.2.
Number of elements: 4,105,459

Fig.A.3. Model used in Section 4.3.
Number of elements: 3,850,342

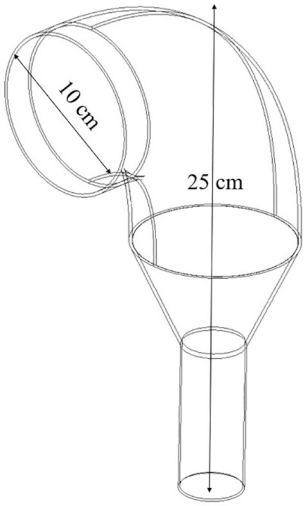

Fig.A.4. Model used in Section 4.4.
Number of elements: 3,768,576

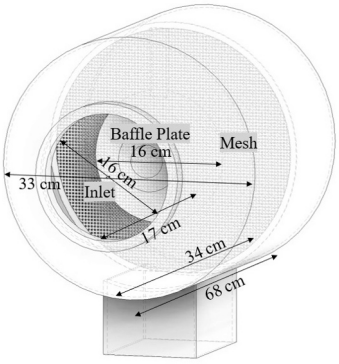

Fig.A.5. Model used in Section 4.5.
Number of elements: 16,755,803

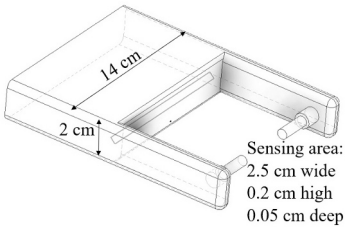

Fig.A.6. Model used in Section 4.7.
Number of elements: 3,505,798

(*continued on next page*)

(*continued*)

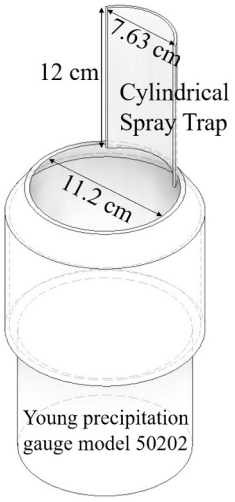

Fig.A.7. Model used in Section 4.8.
Number of elements: 3,673,694

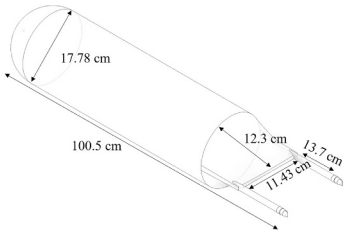

Fig.A.8. Model used in Section 4.9.
Number of elements: 4,830,076

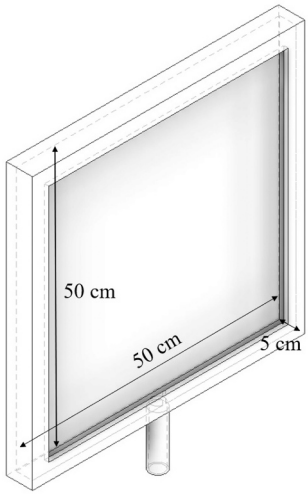

Fig.A.9. Model used in Section 4.10.
Number of elements: 4,443,261

References

Aksyutin, L.R., 1979. Icing of Ships. Sudostroenye Publishing House, Leningrad, p. 126 (in Russian).

Andreas, E.L., 2016. Sea spray generation at a rocky shoreline. Journal of Applied Meteorology and Climatology 55, 2037–2052. https://doi.org/10.1175/JAMC-D-15-0211.1.

Blackmore, R.Z., Lozowski, E.P., 1993. An Heuristic freezing spray model of vessel icing. In: ISOPE-I-93-196. Presented at the the Third International Offshore and Polar Engineering Conference. OnePetro, Singapore.

Bodaghkhani, A., Dehghani, S.-R., Muzychka, Y.S., Colbourne, B., 2016. Understanding spray cloud formation by wave impact on marine objects. Cold Reg. Sci. Technol. 129, 114–136. https://doi.org/10.1016/j.coldregions.2016.06.008.

Borisenkov, Y.P., 1972. On the Theory of Spray Icing of Ships. In: Arkticheskii i Antarkticheskii Nauchno-lssledovatiel skii Institut, Leningrad, pp. 34–43 (in Russian).

Borisenkov, Y.P., Panov, V.V., 1972. Primary results and prospects for the investigation of the hydrometeorological conditions of ship icing. In: Arkticheskii i Antarkticheskii Nauchno-lssledovatiel skii Institut, Trudy No. 298, Gidrometeoizdat, Leningrad, 5-33 (in Russian). Also, USA CRREL Draft Translation 411.

Borisenkov, Y.P., Zablockiy, G.A., Makshtas, A.P., Migulin, A.I., Panov, V.V., 1975. On the approximation of the spray-cloud dimensions. In: Arkticheskii i Antarkticheskii Nauchno-lssledovatiel skii Institut, Trudy No. 317, Gidrometeoizdat, Leningrad, 121-126 (in Russian).

Buyanov, N., 1971. The estimation of icing of a ship. Morskoy Flot 12, 27–28.

Cauteruccio, A., Brambilla, E., Stagnaro, M., Lanza, L.G., Rocchi, D., 2021. Experimental evidence of the wind-induced bias of precipitation gauges using particle image velocimetry and particle tracking in the wind tunnel. J. Hydrol. 600, 126690. https://doi.org/10.1016/j.jhydrol.2021.126690.

Chen, J., Bai, X., Wang, J., Chen, G., Zhang, T., 2022. Research on Sea Spray distribution of Marine Vessels based on SPH-FEM Coupling Numerical simulation Method. Water 14, 3834. https://doi.org/10.3390/w14233834.

Chung, K.K., Lozowski, E.P., Zakrzewski, W.P., Gagnon, R., Thompson, T., 1998. Spraying experiments with a Model Stern Trawler. J. Ship Res. 42, 260–265. https://doi.org/10.5957/jsr.1998.42.4.260.

Chung, V.K.K., 1995. Ship icing and stability (Doctor of Philosophy). University of Alberta, Alberta. https://doi.org/10.7939/R3D50G815.

Colli, M., Lanza, L., 2016. On the wind-induced undercatch in rainfall measurement using CFD-based simulations. In: EGU General Assembly Conference Abstracts EPSC2016-13349.

Colli, M., Lanza, L.G., Rasmussen, R., Thériault, J.M., 2016. The collection efficiency of shielded and unshielded Precipitation Gauges. Part II: modeling particle trajectories. Journal of Hydrometeorology 17, 245–255. https://doi.org/10.1175/JHM-D-15-0011.1.

Colli, M., Pollock, M., Stagnaro, M., Lanza, L.G., Dutton, M., O'Connell, E., 2018. A computational fluid-dynamics assessment of the improved performance of aerodynamic rain Gauges. Water Resour. Res. 54, 779–796. https://doi.org/10.1002/2017WR020549.

Dehghani, S.R., Muzychka, Y.S., Naterer, G.F., 2016a. Droplet trajectories of wave-impact sea spray on a marine vessel. Cold Reg. Sci. Technol. 127, 1–9. https://doi.org/10.1016/j.coldregions.2016.03.010.

Dehghani, S.R., Naterer, G.F., Muzychka, Y.S., 2016b. Droplet size and velocity distributions of wave-impact sea spray over a marine vessel. Cold Reg. Sci. Technol. 132, 60–67. https://doi.org/10.1016/j.coldregions.2016.09.013.

Dehghani, S.R., Naterer, G.F., Muzychka, Y.S., 2018. 3-D trajectory analysis of wave-impact sea spray over a marine vessel. Cold Reg. Sci. Technol. 146, 72–80. https://doi.org/10.1016/j.coldregions.2017.11.016.

Dhar, S., 2021. MarSpray LiDAR (MSL) for the Comprehensive Measurement of Sea Spray for Improving the Prediction of Marine Icing in Cold Conditions (Master thesis). UiT The Arctic University of Norway.

Dhar, S., Khawaja, H.A., 2021. Recognizing potential of LiDAR for comprehensive measurement of sea spray flux for improving the prediction of marine icing in cold conditions - a review. Ocean Eng. 223, 108668. https://doi.org/10.1016/j.oceaneng.2021.108668.

Dhar, S., Samuelsen, E.M., Naseri, M., Aarsæther, K.G., Edvardsen, K., 2022. Spray Icing on ONEGA Vessel- A Comparison of Liquid Water Content Expressions. In: Marine Engineering and Technology II, V05AT06A033. ASME. Presented at the Proceedings of the ASME 2022 41st International Conference on Ocean, Offshore and Arctic Engineering., Hamburg, Germany. https://doi.org/10.1115/OMAE2022-79919.

Fairall, C.W., Banner, M.L., Peirson, W.L., Asher, W., Morison, R.P., 2009. Investigation of the physical scaling of sea spray spume droplet production. J. Geophys. Res. Oceans 114. https://doi.org/10.1029/2008JC004918.

Finstad, K.J., Lozowski, E.P., Makkonen, L., 1988. On the median volume Diameter Approximation for Droplet Collision Efficiency. J. Atmos. Sci. 45, 4008–4012. https://doi.org/10.1175/1520-0469(1988)045<4008:OTMVDA>2.0.CO;2.

Fitzpatrick, J., Stenning, D.G., 1983. Design and construction of Tarsiut Island in the Canadian Beaufort Sea. In: Presented at the Offshore Technology Conference. OnePetro. https://doi.org/10.4043/4517-MS.

Forest, T.W., Lozowski, E.P., Gagnon, R., 2005. Estimating marine icing on offshore structures using RIGICE04. In: Proceedings of the 11th International Workshop on Atmospheric Icing of Structures, June, Montreal, Quebec, Canada.

Fushimi, S., Ozeki, T., Yamaguchi, H., Katsumata, M., Inoue, J., 2019. Sea spray observation and analysis on R/V Mirai. In: Proceedings of the 34th International Symposium on the Okhotsk Sea and Polar Oceans 2019.

Golub'iev, V.N., 1972. On the structure of lee formed due to icing of ships (based on the results of field surveys). Arkticheskii i Antarkticheski i Nauchno-Issledovatielskii Institut, Trudy No. 298, Gidrometeoizdat, 105-115 (in Russian).

Gurvitch, L.Ye, 1972. On the Comparison of Real Ice Loads Due to Icing on the Fishing Vessels with the Regulations of the USSR Registry of Shipping. Arkticheskii i Antarkticheskii Nauchnolssledovatiel ski i lnstitut, Trudy No. 298, Leningrad, Gidrometeoizdat, 137–148 (in Russian).

Hay, R.F.M., 1956. Meteorological aspects of the loss of Lorella and Roderigo. Marine Observation 26, 89–94.

Horjen, I., 1990. Numerical Modeling of Time-Dependent Marine Icing, Anti-icing and De-icing (Doctor thesis). Trondheim University, Norway.

Horjen, I., 2013. Numerical modeling of two-dimensional sea spray icing on vessel-mounted cylinders. Cold Reg. Sci. Technol. 93, 20–35. https://doi.org/10.1016/j.coldregions.2013.05.003.

Horjen, I., 2015. Offshore drilling rig ice accretion modeling including a surficial brine film. Cold Reg. Sci. Technol. 119, 84–110. https://doi.org/10.1016/j.coldregions.2015.07.006.
Horjen, I., Vefsnmo, S., 1984. "Offshore Icing - Phase II - Extended theory os sea spray icing", OTTER Report STF88 F83050, 100 pp.
Horjen, I., Vefsnmo, S., 1987. Time-dependent Sea Spray Icing on Ships and Drilling Rigs — A Theoretical Analysis. Offshore Icing — Phase IV, NHL-report STF60 F87130 (87 pp.).
Horjen, I., Løset, S., Vefsnmo, S., 1986. Icing hazards on supply vessels and stand-by boats. Report number: STF60 A 86073, NHL (now SINTEF).
Houghton, E.L., Carpenter, P.W., Collicott, S.H., Valentine, D.T., 2017. Chapter 5 - Potential Flow. In: Houghton, E.L., Carpenter, P.W., Collicott, S.H., Valentine, D.T. (Eds.), Aerodynamics for Engineering Students, Seventh ed. Butterworth-Heinemann, pp. 329–389. https://doi.org/10.1016/B978-0-08-100194-3.00005-5.
Itagaki, K., 1977. Icing on Ships and Stationary Structures under Maritime Conditions. A Preliminary Literature Survey of Japanese Sources. (No. ADA044792). Cold Regions Research and Engineering Laboratory, New Hampshire.
Itagaki, K., 1984. Icing Rate on Stationary Structures under Marine Conditions (Report No. CRREL Report 84-12.), This Digital Resource was created from scans of the Print Resource. Cold Regions Research and Engineering Laboratory (U.S.).
Jones, K.F., Andreas, E., 2013. Winter Measurements of Sea Spray at Mt. Desert Rock. In: Proceedings of the 15th International Workshop on Atmospheric Icing of Structures (IWAIS XV), At: St. John's, Newfoundland, Canada.
Jones, K.F., Andreas, E.L., 2014. Sea Spray and Icing in the Emerging Open Water of the Arctic Ocean (Annual report No. ADA617969). U.S. Army Corps of Engineers, Cold Regions Research and Engineering Laboratory.
Jones, K.F., Thompson, G., Claffey, K.J., Kelsey, E.P., 2014. Gamma distribution parameters for cloud drop distributions from multicylinder measurements. J. Appl. Meteorol. Climatol. 53, 1606–1617. https://doi.org/10.1175/JAMC-D-13-0306.1.
Jorgensen, T.S., 1983. Results from Laboratory Studies of Photo-Technique as a Tool for Measurements of Droplet Sizes. Suggestion for Equipment. (In Norwegian). OTTER-memo No 1730, NHL (now SINTEF).
Jorgensen, T.S., 1984. Sea spray measurements on the drilling rig 'Treasure Scout'. OTTER-Report No. STF88 F84038, NHL (now SINTEF) (In Norwegian).
Jorgensen, T.S., 1985. Sea spray measurements on the drilling rig 'Treasure Scout'. Tech. Rep. STF60 F 85015, NHL (now SINTEF).
Jorgensen, T.S., 1986. Offshore Icing - phase II Final report. Technical report, NHL (now SINTEF).
Kultashev, Ye.N., Panov, V.V., 1970. Results of investigations of icing on ships under environmental conditions. In: Technology of Naval Architecture, No. 1. Sudostroenye Publishing House, Leningrad (in Russian).
Kultashev, Ye.N., Malakhov, N.F., Panov, V.V., Shmidt, M.V., 1972. Spray icing of medium-sized fishing vessels and medium-sized freezing trawlers. In: Arkticheskii i Antarkticheskii Nauchno-lssledovatie'skii lnstitut, Trudy No. 298, Leningrad, Gidrometeoizdat, Leningrad, 125–136 (in Russian). Also, USA CRREL Draft Trans lat ion No. 411.
Kulyakhtin, A., Kulyakhtin, S., Løset, S., 2016. The role of the ice heat conduction in the ice growth caused by periodic sea spray. Cold Reg. Sci. Technol. 127, 93–108. https://doi.org/10.1016/j.coldregions.2016.04.001.
Kuznietsov, V.P., Kultashev, Ye.N., Panov, V.V., Tyurin, A.P., Sharapov, A.V., 1971. Environmental investigations of icing of ships in the Japan Sea in 1969. In: Theoretical and experimental investigations of conditions of icing on ships. Arkticheskii i Antarkticheskii Nauchno-lssledovatiel'skii lnstitut. Gidrometeorologicheskoye lzdatiel'stvo, Leningrad, pp. 57–69 (in Russian).
Lai, R.J., Shemdin, O.H., 1974. Laboratory study of the generation of spray over water. J. Geophys. Res. 79, 3055–3063. https://doi.org/10.1029/JC079i021p03055.
Lennox, E.R., Kreisberg, N.M., Montoya, L.D., 2013. Design and characterization of a new coarse particle collector based on microtrap impactor technology. Aerosol Sci. Tech. 47, 626–633. https://doi.org/10.1080/02786826.2013.778385.
Lozowski, E.P., Zakrzewski, W.P., 1993. Topside Ship Icing System. Cold Regions Research and Engineering Laboratory.
Lozowski, E.P., Szilder, K., Makkonen, L., 2000. Computer simulation of marine ice accretion. Philosophical transactions of the Royal Society of London. Series a: Mathematical. Phys. Eng. Sci. 358, 2811–2845. https://doi.org/10.1098/rsta.2000.0687.
Lozowski, E.P., Forest, T.W., Chung, V., Szilder, K., 2002. Study of Marine Icing: Final Report. NRC. Institute for Ocean Technology. Contractor Report Panel on Energy Research and Development (PERD) PanCanadian/EnCana NRC Institute for Ocean Technology Canada, 5415. https://doi.org/10.4224/8896262.
Menter, F., Kuntz, M., Langtry, R., 2003. Ten years of industrial experience with the SST turbulence model. Heat Mass Transf. 4.
Menter, F.R., 1994. Two-equation eddy-viscosity turbulence models for engineering applications. AIAA J. 32, 1598–1605. https://doi.org/10.2514/3.12149.
Minsk, L.D., 1984. Assessment of Ice Accretion on Offshore Structures (no. 84–4). Cold Regions Research and Engineering Lab Hanover NH.
Mintu, S., Molyneux, D., 2022. Ice accretion for ships and offshore structures. Part 2 – Compilation of data. Ocean Engineering 248, 110638. https://doi.org/10.1016/j.oceaneng.2022.110638.
Mintu, S., Molyneux, D., Colbourne, B., 2019. Multi-phase simulation of droplet trajectories of wave-impact sea spray over a vessel. In: Proceedings of the ASME 2019 38th International Conference on Ocean, Offshore and Arctic Engineering. Presented at the OMAE 2019, Glasgow, Scotland, UK. https://doi.org/10.1115/OMAE2019-95799.
Mintu, S., Molyneux, D., Colbourne, B., 2021a. A theoretical model for Ship–Wave impact generated sea spray. J. Offshore Mech. Arct. Eng 143. https://doi.org/10.1115/1.4049122.
Mintu, S., Molyneux, D., Colbourne, B., 2021b. Full-scale SPH simulations of ship-wave impact generated sea spray. Ocean Eng. 241, 110077. https://doi.org/10.1016/j.oceaneng.2021.110077.
Monahan, E.C., 1968. Sea spray as a function of low elevation wind speed. J. Geophys. Res. 73, 1127–1137. https://doi.org/10.1029/JB073i004p01127.
Montecinos, S., Carvajal, D., Cereceda, P., Concha, M., 2018. Collection efficiency of fog events. Atmos. Res. 209, 163–169. https://doi.org/10.1016/j.atmosres.2018.04.004.
Muzik, I., Kirby, A., 1992. Spray overtopping rates for Tarsiut Island: model and field study results. Can. J. Civ. Eng. 19, 469–477. https://doi.org/10.1139/l92-057.
NTSB, 2018. Capsizing and Sinking of Fishing Vessel Destination (Marine accident report No. DCA17FM006). National Transportation Safety Board.
NTSB, 2020. Capsizing and Sinking of Commercial Fishing Vessel Scandies Rose (Marine accident report No. MAR-21/02). National Transportation Safety Board.
Ozeki, T., Shiga, T., Sawamura, J., Yashiro, Y., Adachi, S., Yamaguchi, H., 2016a. Development of Sea Spray Meters and an Analysis of Sea Spray Characteristics in large Vessels. In: Proceedings of the Twenty-Sixth (2016) International Ocean and Polar Engineering Conference. Presented at the International Society of Offshore and Polar Engineers (ISOPE). Rhodes, Greece, OnePetro.
Ozeki, T., Shiga, T., Sawamura, J., Yashiro, Y., Adachi, S., Yamaguchi, H., 2016b. Development of sea spray meters and an analysis of sea spray characteristics in large vessels. In: Proceedings of the Twenty-Sixth (2016) International Ocean and Polar Engineering Conference.
Ozeki, T., Yashiro, Y., Sagawa, G., Tateyama, K., Toyota, T., 2016c. Field Observations of Impinging Seawater Spray Using Sea Spray Meters. In: Proceedings of the 31st International Symposium on Okhotsk Sea & Sea Ice.
Ozeki, T., Toda, S., Yamaguchi, H., 2018. An Investigation on the Feature of Seawater Spray Impinging on the R/V Mirai. In: Proceedings of the Twenty-Eighth (2018) International Ocean and Polar Engineering Conference. Presented at the International Society of Offshore and Polar Engineers (ISOPE), Sapporo, Japan.
Panitz, T., Wasan, D.T., 1972. Flow attachment to solid surfaces: the Coanda effect. AICHE J. 18, 51–57. https://doi.org/10.1002/aic.690180111.
Panov, V.V., 1971. On the frequency of splashing the medium fishing vessel with sea spray. In: Theoretical and Experimental Investigations of the Conditions of Icing of Ships (in Russian). Gidrometeoizdat Leningrad.
Panov, V.V., 1976. Icing of ships. In: Arktlcheskii i Antarkticheskii Nauchno-lssledovatiel'skii lnstitut, Trudy No. 334, Gldrometeoizdat, Leningrad, p. 263 (in Russian).
Pollock, M.D., O'Donnell, G., Quinn, P., Dutton, M., Black, A., Wilkinson, M.E., Colli, M., Stagnaro, M., Lanza, L.G., Lewis, E., Kilsby, C.G., O'Connell, P.E., 2018. Quantifying and Mitigating Wind-Induced Undercatch in Rainfall Measurements. Water Resour. Res. 54, 3863–3875. https://doi.org/10.1029/2017WR022421.
Preobrazhenskii, Ly, 1973. Estimate of the content of spray-drops in the near-water layer of the atmosphere. Fluid Mech. Soviet Res. 2, 95–100.
Roebber, P., Mitten, P., 1987. Modelling and measurement of icing in Canadian waters (No. Report (Canadian Climate Centre), nos. 87–15.). Atmospheric Environment Service, Canada, Ontario.
Rozenberg, V.B., 1971. Statistical analyses of icing on fishing vessels. In: Analysis of ship disasters for fishing industrial vessels and recommendations. Leningrad, lzdatiel'stvo Transport, Vol. 21, pp. 32–36 (in Russian).
Ryerson, C.C., 1995. Superstructure spray and ice accretion on a large U.S. Coast Guard cutter. Atmospheric Research, Atmospheric Icings of Structures 36, 321–337. https://doi.org/10.1016/0169-8095(94)00045-F.
Ryerson, C.C., Longo, P.D., 1992. Ship superstructure icing data collection and instrument performance on USCGC Midgett Research Cruise (Report), This Digital Resource was created from scans of the Print Resource. Cold Regions Research and Engineering Laboratory (U.S.).
Samuelsen, E.M., 2017. Prediction of Ship Icing in Arctic Waters - Observations and Modelling for Application in Operational Weather Forecasting (Doctoral Thesis). Faculty of Science and Technology Department of Engineering and Safety IVT. UiT Norges arktiske universitet, Norway.
Samuelsen, E.M., Graversen, R.G., 2019. Weather situation during observed ship-icing events off the coast of Northern Norway and the Svalbard archipelago. Weather and Climate Extremes 24, 100200. https://doi.org/10.1016/j.wace.2019.100200.
Samuelsen, E.M., Edvardsen, K., Graversen, R.G., 2017. Modelled and observed sea-spray icing in Arctic-Norwegian waters. Cold Reg. Sci. Technol. 134, 54–81. https://doi.org/10.1016/j.coldregions.2016.11.002.
Sapone, D.T., 1990. A Sensitivity Study of Bow Variants on the Distribution of Sea Spray in Regular Head Seas (Thesis). Massachusetts Institute of Technology.
Sharapov, A.V., 1971. On the intensity of lee build-up on ships (of MFV type). In: Theoretical and experimental investigations of conditions-of icing on ships. Arkticheskii i Antarkticheskii Nauchno-lssledovatiel ski i lnstitut, Leningrad, Gidrometeolzdat, pp. 95–97 (in Russian).
Shellard, H.C., 1974. The Meteorological Aspects of Ice Accretion on Ships (No. Marine Science Affairs Report NO. 10.). World Meteorological Organization, Switzerland.
Shiga, T., Ozeki, T., Sawamura, J., Yamaguchi, H., 2015. Analysis of sea spray characteristics in large vessels - Case study of the icebreaker Shirase. In: Presented at the 30th International Symposium on Okhotsk Sea & Sea Ice, Mombetsu, Hokkaido, Japan, pp. 147–150.
Smirnov, V.I., 1972. Conditions of ship icing and anti-icing techniques (according to foreign data). In: Arkticheskii i Antarkticheskii Nauchno-lssledovatiel ski i Institut, Trudy No. 298, Gidrometeoizdat, Leningrad, 174-178 (in Russian). Also, USA CRREL Draft Translation 411.
Stokes, G.G., 1851. On the effect of internal friction of fluids on the motion of pendulums. Transactions of the Cambridge Philosophical Society 9, 8–106.

Sultana, K.R., Dehghani, S.R., Pope, K., Muzychka, Y.S., 2018. A review of numerical modelling techniques for marine icing applications. Cold Reg. Sci. Technol. 145, 40–51. https://doi.org/10.1016/j.coldregions.2017.08.007.

Tabata, T., 1969. Studies on the ice accumulation on ships. III. relation between the rate of ice accumulation and air, sea conditions. Low Temperature Science Ser. A 27, 339–349 (In Japanese).

Teigen, S.H., Ekeberg, O.-C., Myhre, B., Rustad, H., Petersen, S., Schrøder-Bråtane, E., Carlsen, S., 2019. Autonomous Real-Time Sea Spray Measurement System for Offshore Structures. In: Proceedings of the International Conference on Port and Ocean Engineering Under Arctic Conditions. Presented at the 25th International Conference on Port and Ocean Engineering under Arctic Conditions (POAC 2019).

Thomas, W.L., 1991. Bering Sea Topside Icing Probabilities for Two Naval Combatants. David Taylor Research Center, Bethesda, MD.

Toba, Y., 1962. Drop Production by Bursting of Air Bubbles on the Sea Surface - Study by Use of a Wind Flume (Doctoral Thesis). Kyoto University.

Venturi, G.B., 1797. Recherches expérimentales sur le principe de la communication latérale du mouvement dans les fluides, etc. chez Houel et Ducros.

Veron, F., 2015. Ocean Spray. Annu. Rev. Fluid Mech. 47, 507–538. https://doi.org/10.1146/annurev-fluid-010814-014651.

Walsh, M.R., Morse, J.S., Knuth, K.V., Lambert, D.J., 1992. Ship icing instrumentation (Report), This Digital Resource was created from scans of the Print Resource. Cold Regions Research and Engineering Laboratory (U.S.).

Weller, R.A., 2018. Observing Surface Meteorology and Air-Sea Fluxes. In: Venkatesan, R., Tandon, A., D'Asaro, E., Atmanand, M.A. (Eds.), Observing the Oceans in Real Time. Springer Oceanography. Springer International Publishing, Cham, pp. 17–35. https://doi.org/10.1007/978-3-319-66493-4_2.

Wu, J., 1990. On parameterization of sea spray. J. Geophys. Res. Oceans 95, 18269–18279. https://doi.org/10.1029/JC095iC10p18269.

Wu, J., Murray, J.J., Lai, R.J., 1984. Production and distributions of sea spray. J. Geophys. Res. 89, 8163. https://doi.org/10.1029/JC089iC05p08163.

Zakrzewski, W.P., 1986. Icing of Ships. Part I, Splashing a Ship with Spray (Technical Report NOAA Technical Memorandum ERL PMEL~66). NOAA – National Oceanic and Atmospheric Administration, Seattle, Washington, USA.

Zakrzewski, W.P., 1987. Splashing a ship with collision-generated spray. Cold Reg. Sci. Technol. 14, 65–83. https://doi.org/10.1016/0165-232X(87)90045-0.

Zakrzewski, W.P., Lozowski, E.P., 1989. Soviet marine icing data. Atmospheric Environment ServiceCanadian Climate Centre Report. 89–2, p. 125. Ontario.